Run I ATLAS Results on Heavy Ion Collisions

Helena Santos, LIP

LIP Seminar, 30th April 2014

Heavy Ion Physics

- Systematic study of a hot, dense and strongly coupling systems

- Extending our understanding of QCD by studying distinct phases of matter: hadronic vs. partonic deconfined system (Plasma of Quarks and Gluons)

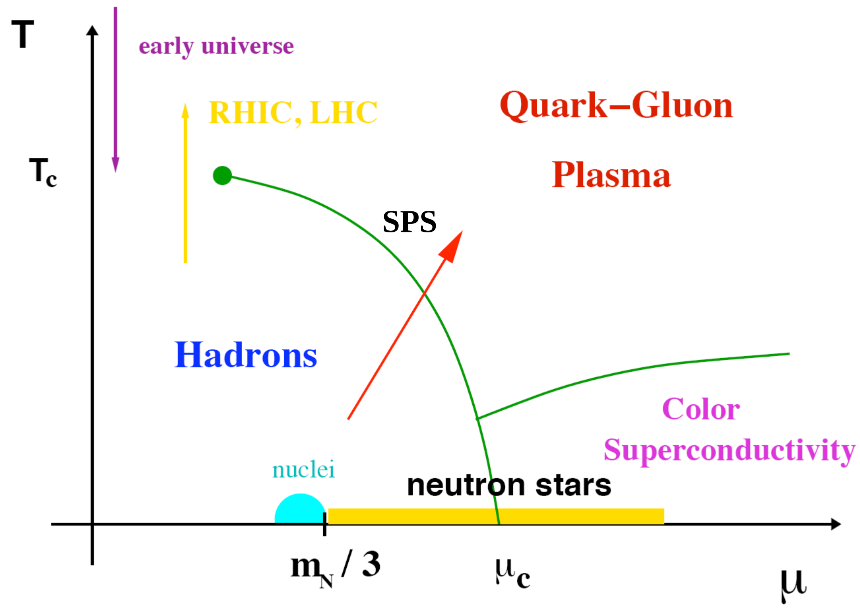

$\sqrt{s}$: 17 GeV@SPS 200 GeV@RHIC 2.76 TeV@LHC

Colliding nuclei: Pb+Pb Au+Au Pb+Pb

What have we learnt from Pb+Pb and p+Pb collisions at LHC?

Global observables:

- Charged multiplicity
- Particle flow
- Particle correlations

Hard probes:

- EW
- Jets

Run I

Year	Species	$\sqrt{s_{NN}}$ [TeV]	L_{int} [nb^{-1}]
2010	Pb+Pb	2.76	0.01
2011	p+p	2.76	300
2011	Pb+Pb	2.76	0.15
2012	p+Pb	5.02	0.001
2013	p+Pb	5.02	30
2013	p+p	2.76	5000

Soft sector provides measurements of bulk properties.

Hard probes provide access to initial state effects (shadowing, EMC, initial E-loss) via Z/W/photons and to final state effects via jet suppression.

ATLAS Acceptance

Full azimuthal coverage

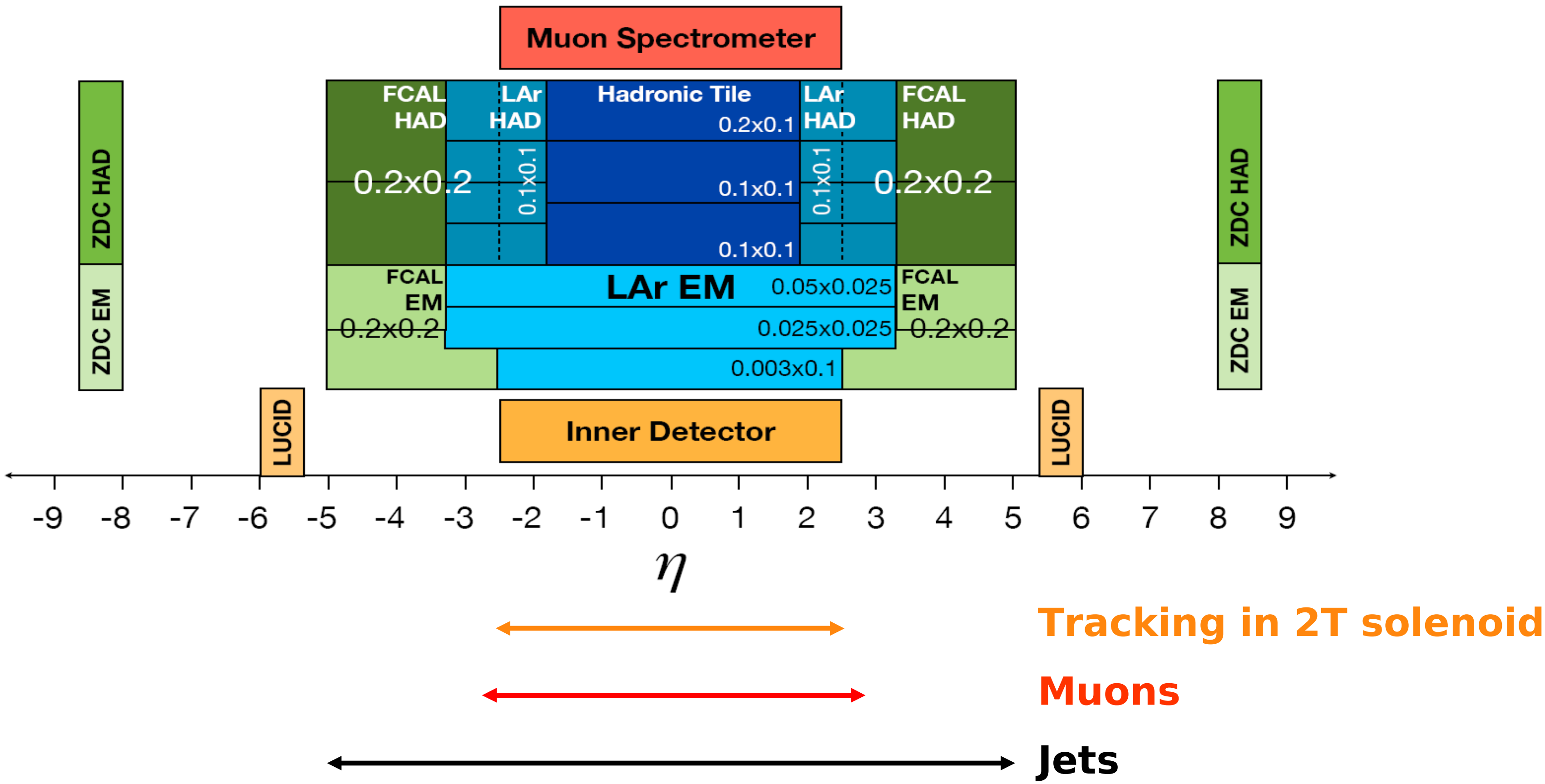

$x_1 \sim (2p_T/\sqrt{s})e^{\eta}$

Forward coverage provides access to:

$x_2 \sim (2p_T/\sqrt{s})e^{-\eta}$

Collision's Centrality

ATLAS Calorimeter System

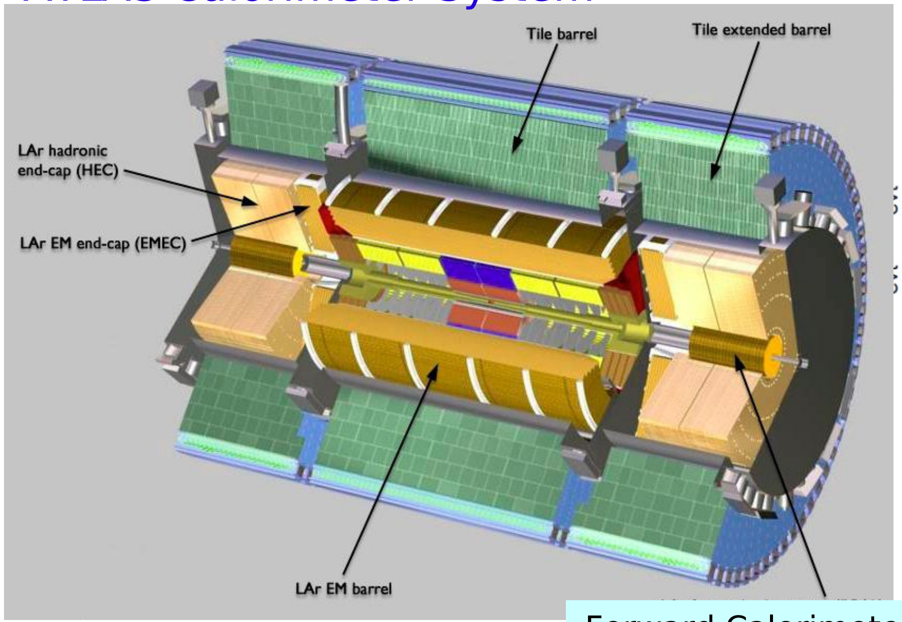

Forward Calorimeter
3.2<|η|<4.9

E_T in Forward Calorimeter

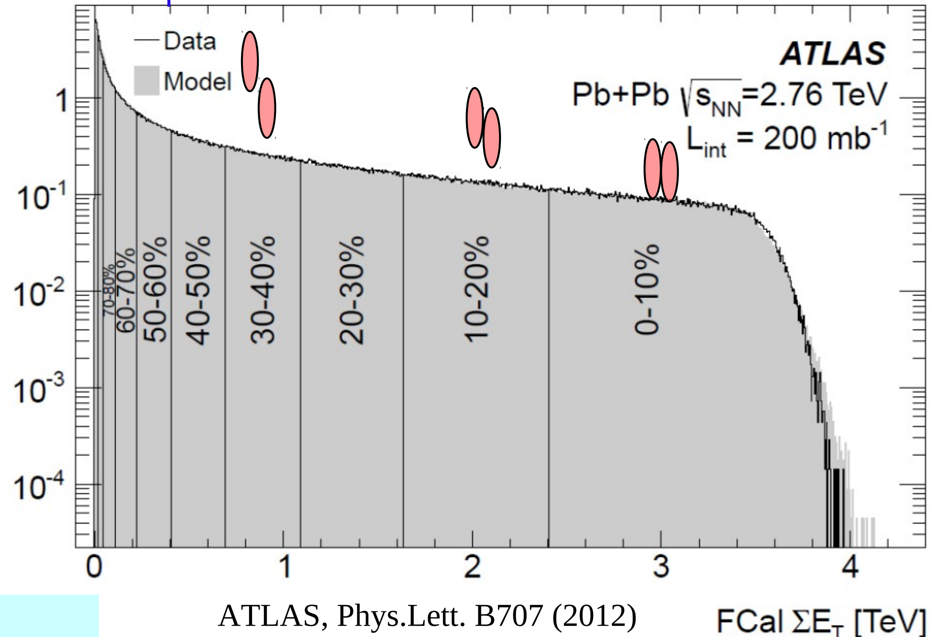

ATLAS, Phys.Lett. B707 (2012) 330-348

- Transverse energy in FCal compared to Glauber MC model
- 98 ± 2% of inelastic collisions after trigger and selection cuts
- <N_{part}> and <N_{coll}> for each centrality bin are estimated using the same Glauber

Global observables

Global variables (multiplicity, correlations and flow) are integrals of particle number and energy in final state but reflect dynamical quantities, as entropy and transverse energy, established much earlier in the system evolution.

Hidrodynamic evolution of the system

Phys.Rev.Lett.106, 042301 (2011)

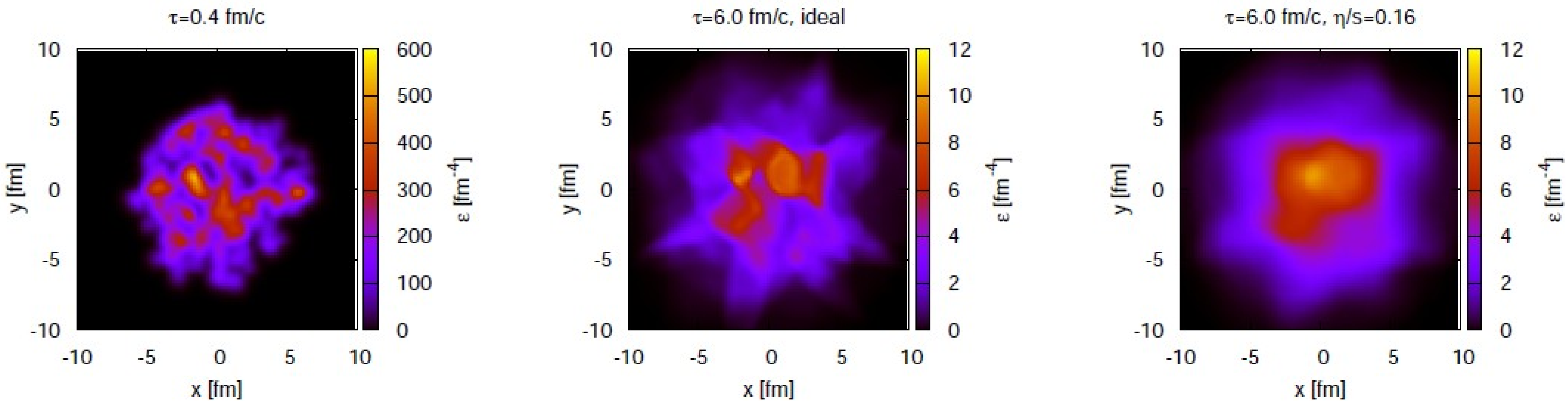

Initial

after 6 fm/c

Low η/s means strong coupling

Tracking Methods

Global variables are measured with charged particles in ID (Pixel + SCT)

- Selected track p_T > 0.5 GeV (0 in case of multiplicity)
- -2.5 < η < 2.5
- Full φ acceptance
- Tighter track selection cuts than in p+p

ATLAS Inner Detector (ID)

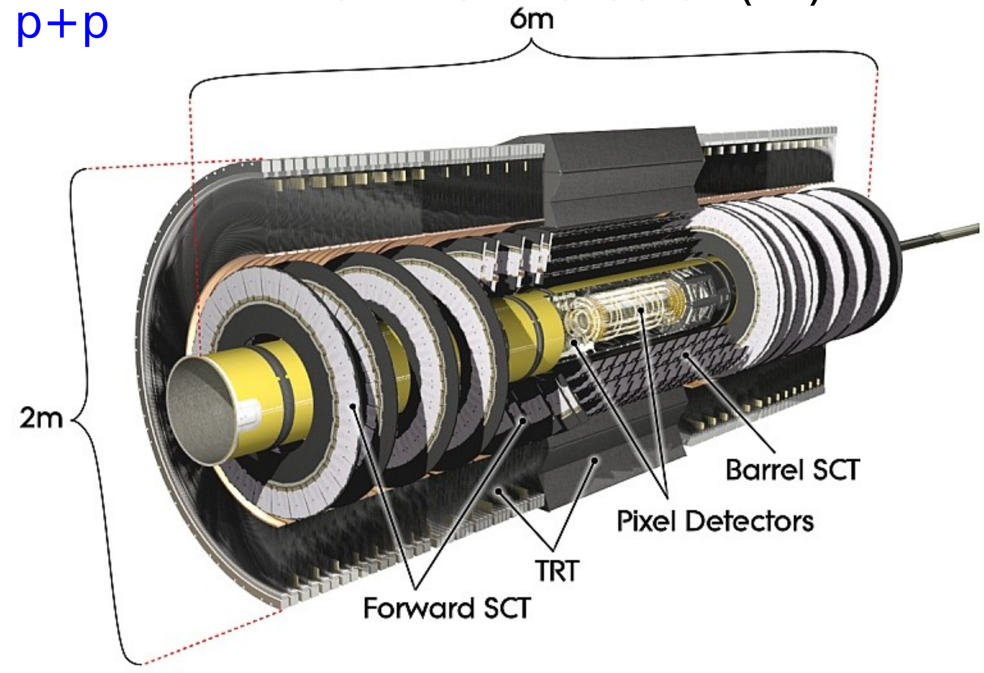

Two tracking methods used:

1 – Kalman Filter based tracking algorithm - ATLAS standard

2 - “Two-point tracklets”

Select cluster pairs aligned with primary vertex

Charged Particle Multiplicity

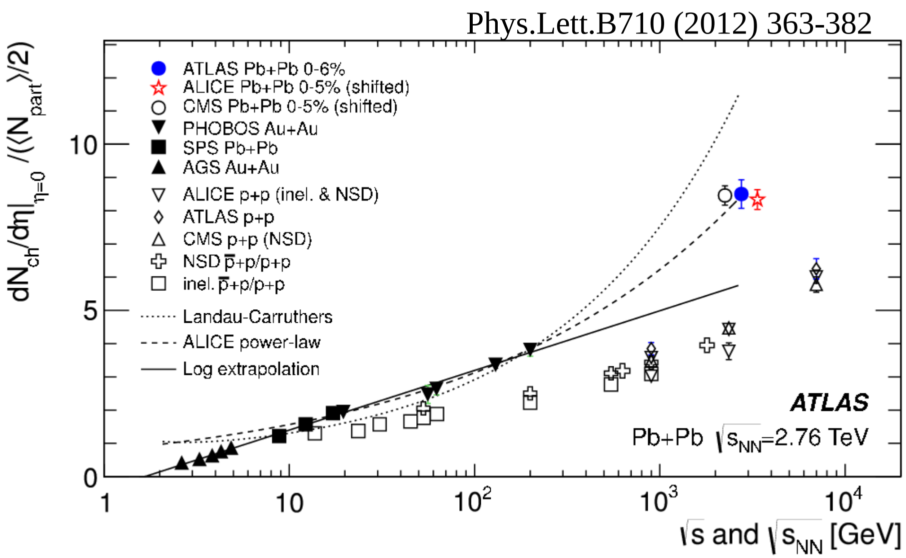

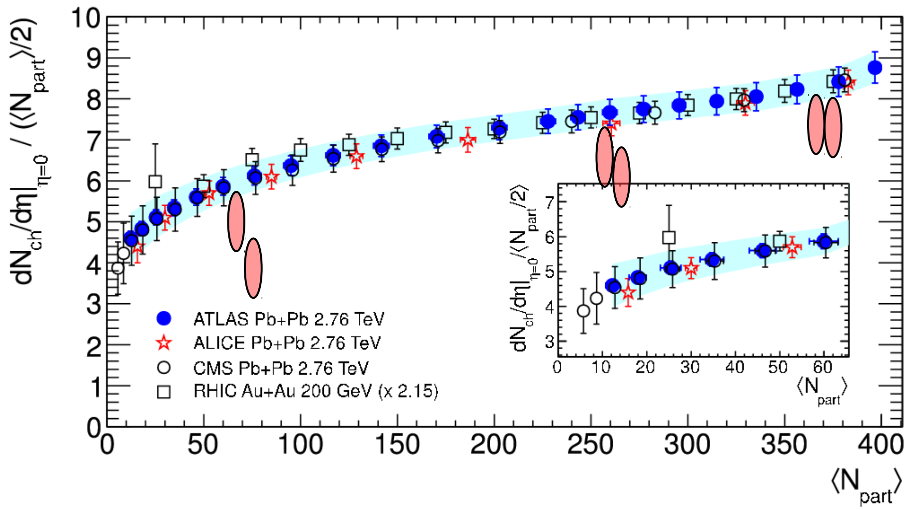

- Yield per participant pair increases by factor of two relative to RHIC, in agreement with ALICE and CMS measurements (shifted for clearness)
- Charged particle multiplicity by nucleon pair follows a power law
- Twice more particles per participant pair compared to p+p
- Variation with centrality consistent between LHC and RHIC (scaled by 2.15)

Multiplicity in Pb+Pb Collisions

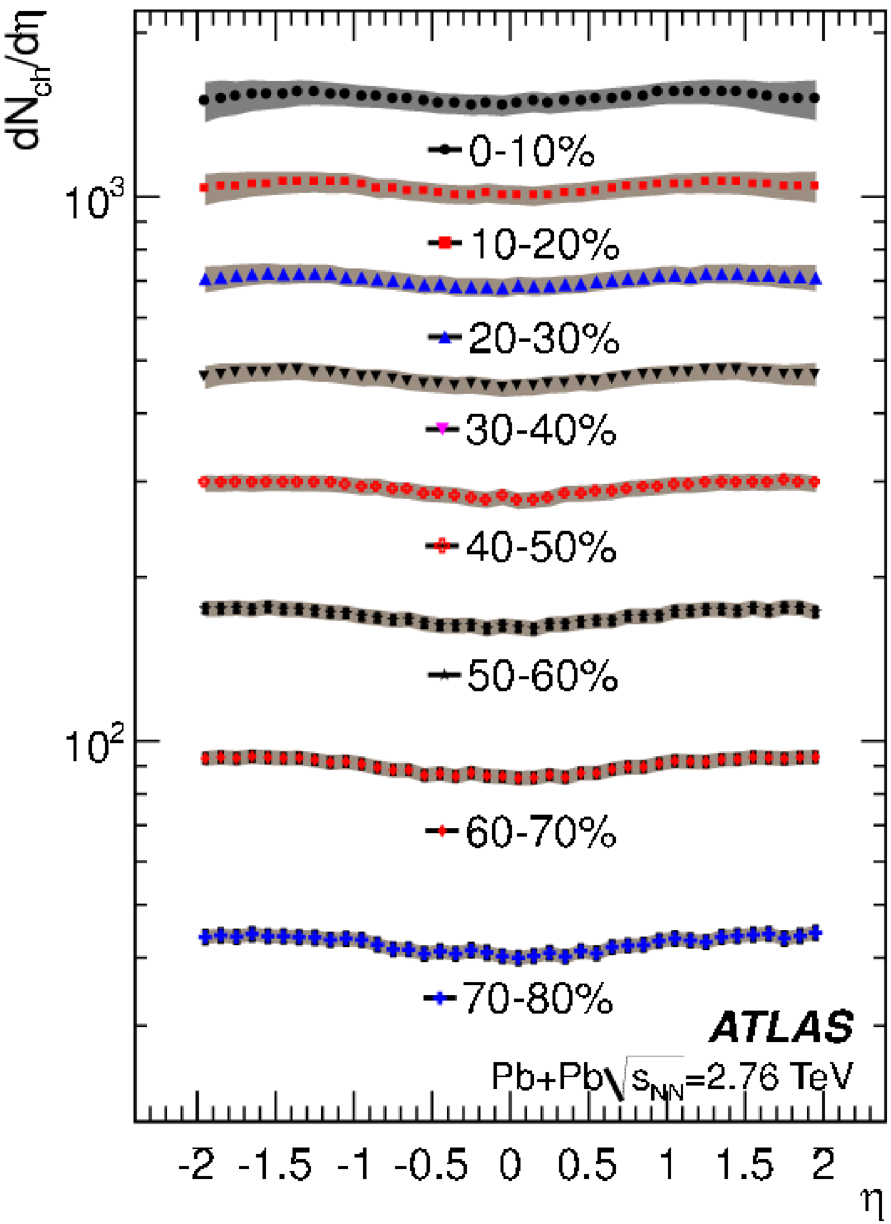

Phys.Lett.B710 (2012) 363-382

Up to 8,000 charged particles in ATLAS tracking at $\sqrt{s_{NN}}$=2.76 TeV

Flat in rapidity within |η|<2, similar to p+p

Multiplicity in p+Pb collisions

ATLAS-CONF-2013-096

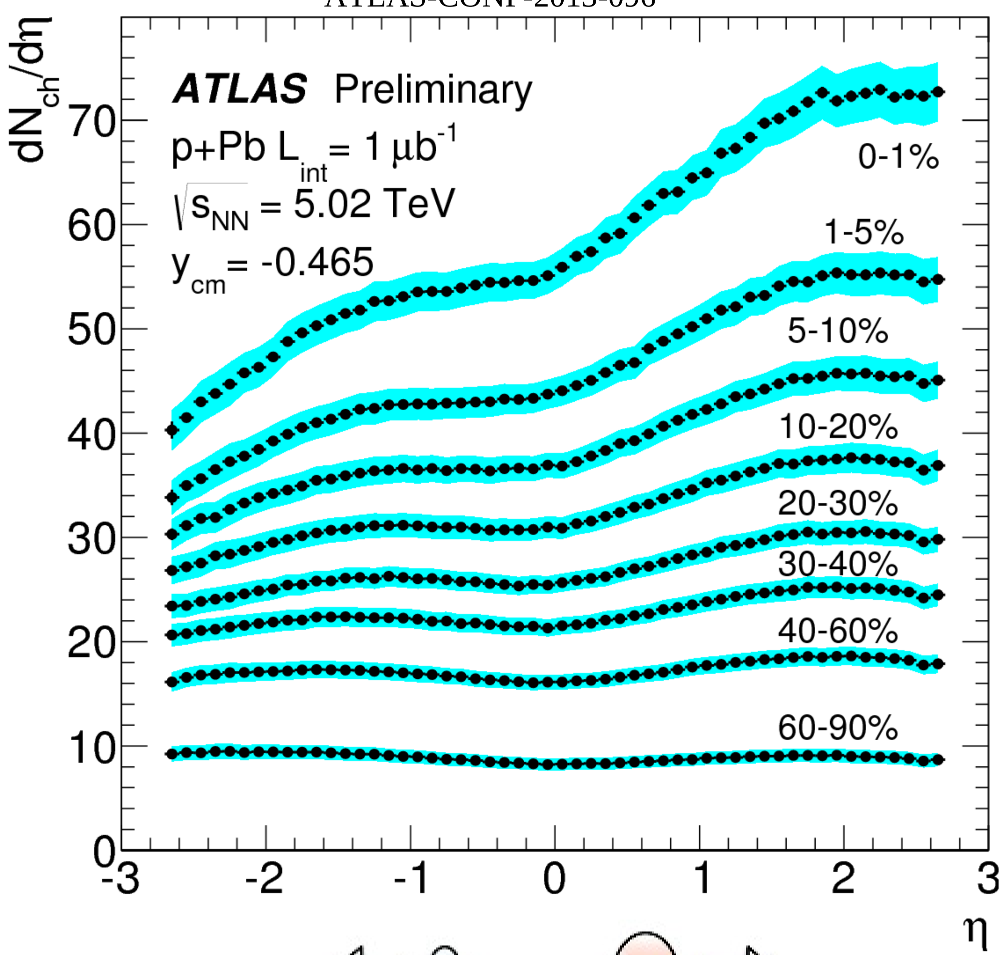

60-90% - double peak structure similar to Pb+Pb and p+p.

Forward-backward asymmetry between p and going directions increases with collision's centrality.

Baseline to understand Pb+Pb collisions.

Azymuthal Anisotropic Flow - I

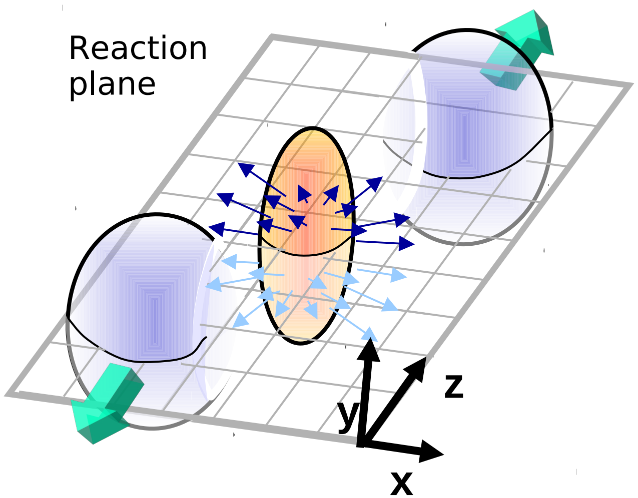

Anisotropic spatial collective motion is described by a Fourier expansion of particle distribution in azimuthal angle φ

$$\frac{dN}{d\phi} \propto 1 + 2\sum_{n=1}^{\infty} v_n \cos n(\phi - \Phi_n)$$

- v_n and Φ_n represent the magnitude and phase of the n^{th} order anisotropy in the momentum space
- Reaction plane is defined by the impact parameter between the two nuclei and the beam axis

Azymuthal Anisotropic Flow - II

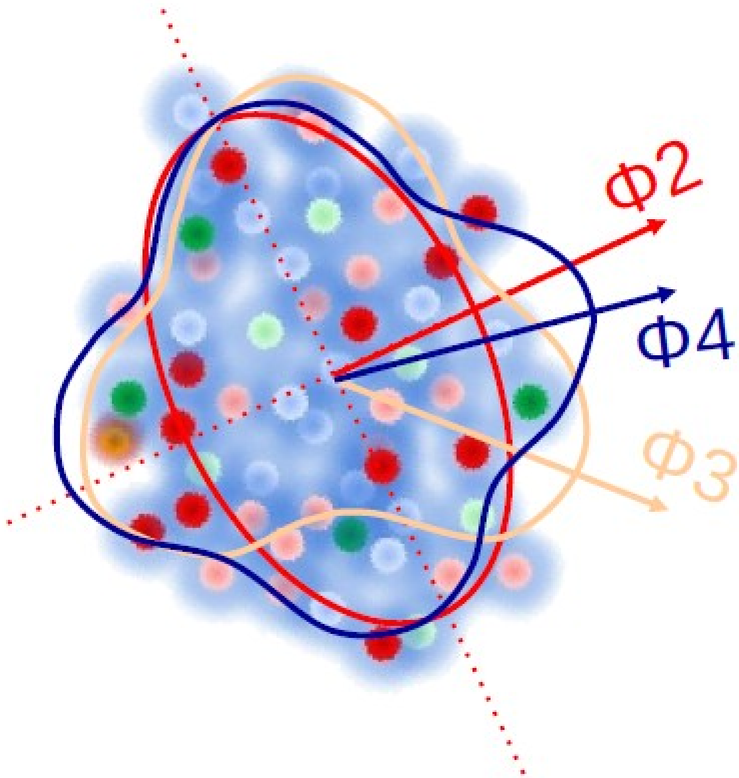

v_2 is associated with elliptic shape of nuclear overlap

Higher order coefficients are associated with fluctuations of nucleon positions in the overlap

$$\frac{\mathrm{d}N}{\mathrm{d}\phi} \propto 1 + 2\sum_{n=1}^{\infty} v_n \cos n(\phi - \Phi_n)$$

Signicant values of the higher order harmonics, v_3 - v_6, are consistent with small η/s and imply large event-by-event flow vector fluctuations

$$\vec{v}_n = (v_n \cos n\Phi_n, v_n \sin n\Phi_n)$$

Event-by-Event Fluctuations

JHEP11(2013)183

Single track azimuthal distributions in central collisions

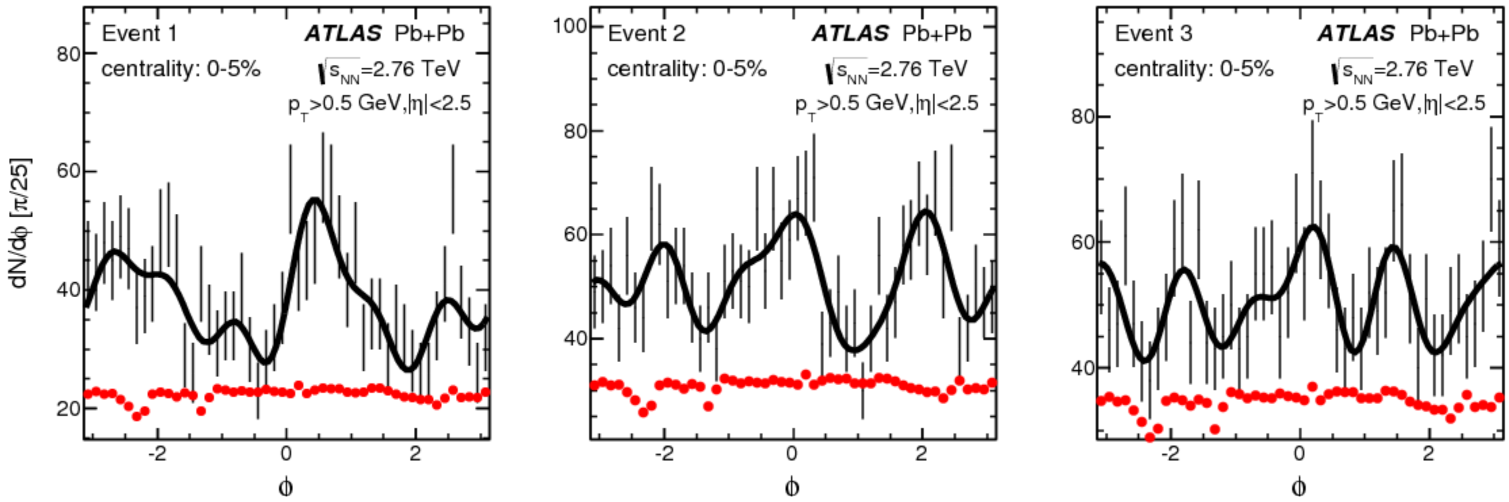

Significant fluctuations, factor of ~2

Cannot be explained by detector effects

Shall be corrected for efficiency, acceptance and finite multiplicity

Red distributions are event-averaged

v_n probability distributions

$$p(\vec{v}_n) = \frac{1}{2\pi\delta_{v_n}^2} e^{-(\vec{v}_n - \vec{v}_n^{\,\mathrm{RP}})^2/(2\delta_{v_n}^2)}$$

JHEP11(2013)183

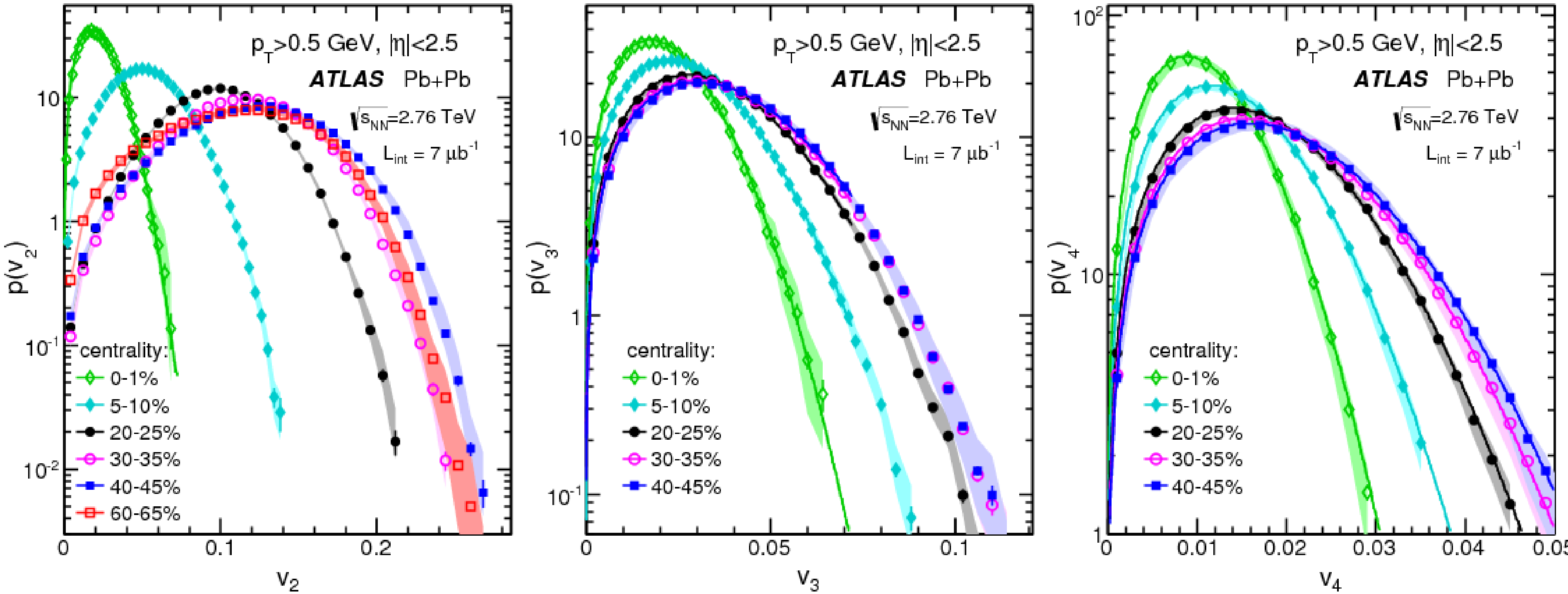

$p(v_n)$ are integration over Φ of 2D Gaussians

Shaded bands are uncertainties on v_n shape

Solid curves in v_2 (central), v_3 and v_4 represent fluctuations-only scenario

v_2 - Comparison to Models

Eccentricity of initial geometry from MC Glauber and KLN models

$$\epsilon_n = \frac{\sqrt{\langle r^n \cos n\phi \rangle^2 + \langle r^n \sin n\phi \rangle^2}}{\langle r^n \rangle}$$

JHEP11(2013)183
nucl-ex/0701024
Phys. Rev. C74, 044905 (2006)

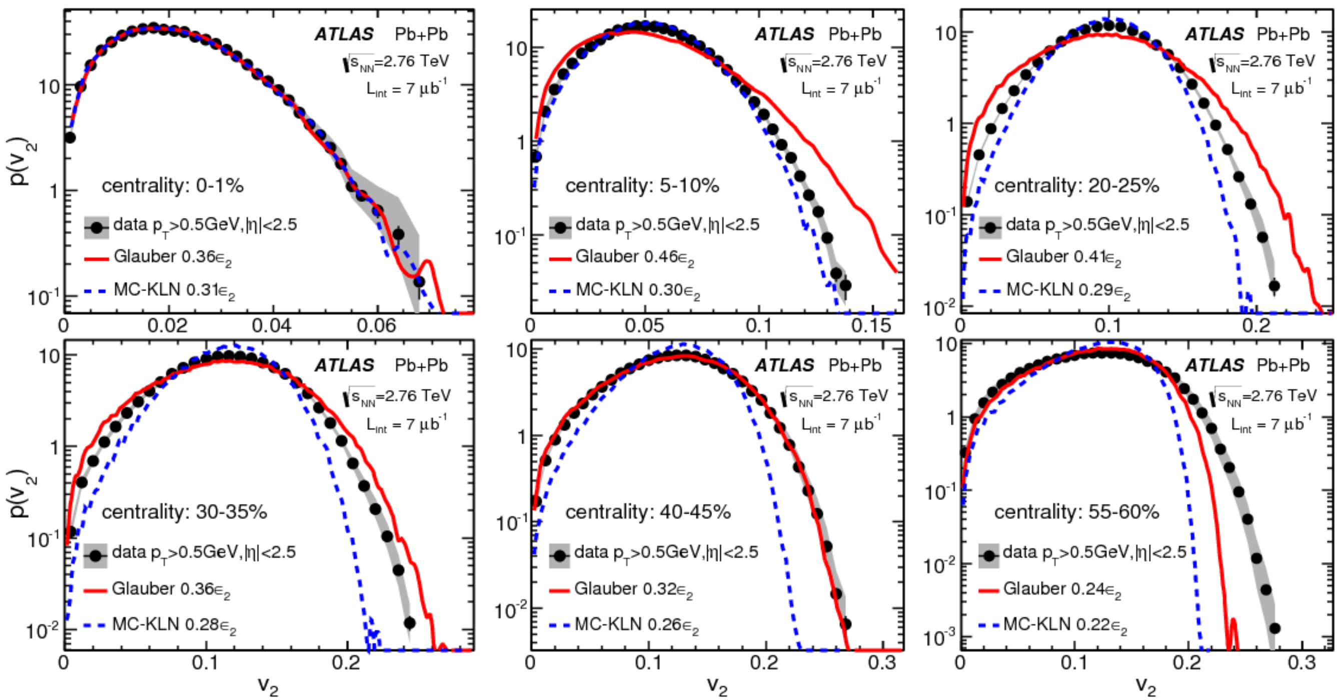

Both work in 0-1%

Both fail in 55-60%

MC KLN better in 5-10%

MC Glauber better in 30-45%

2-Particle Correlations in p+Pb

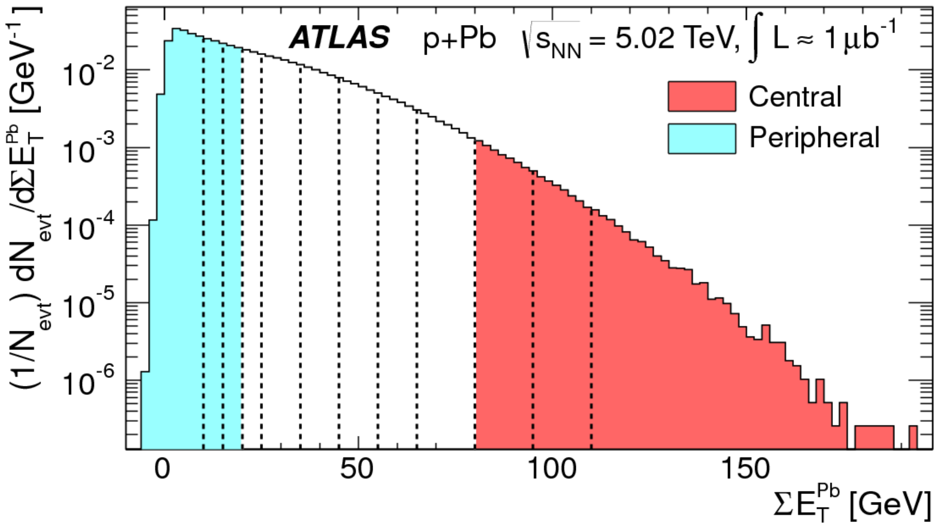

Phys. Rev. Lett. 110, 182302 (2013)

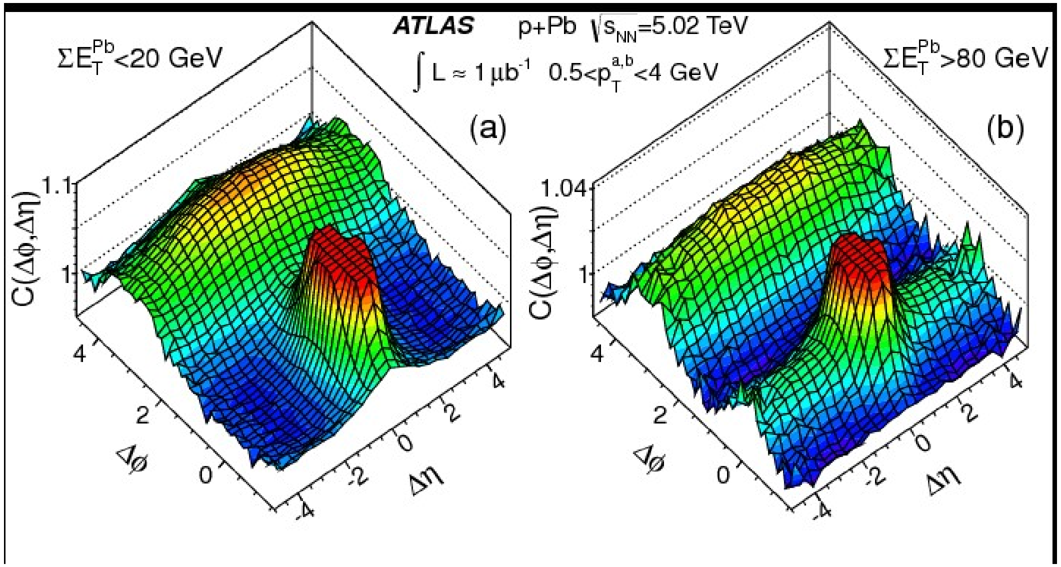

$$C(\Delta\phi, \Delta\eta) = \frac{S(\Delta\phi, \Delta\eta)}{B(\Delta\phi, \Delta\eta)}$$

S(Δη,Δφ) is the same-event pair

B(Δη,Δφ) is the combinatorial background pair

- Sharp peak at (Δη,Δφ)=(0,0) due to pairs originating from the same jet, Bose-Einstein correlations, resonance decays.
- Structure at Δφ=π due to dijets, low p_T resonances and momentum conservation.

2-Particle Correlations in Pb+Pb

Phys. Rev. C 86, 014907 (2012)

$$C(\Delta\phi,\Delta\eta)=\frac{S(\Delta\phi,\Delta\eta)}{B(\Delta\phi,\Delta\eta)}$$

S(Δη,Δφ) is the same-event pair

B(Δη,Δφ) is the combinatorial background pair

- Long and short range structures in central events

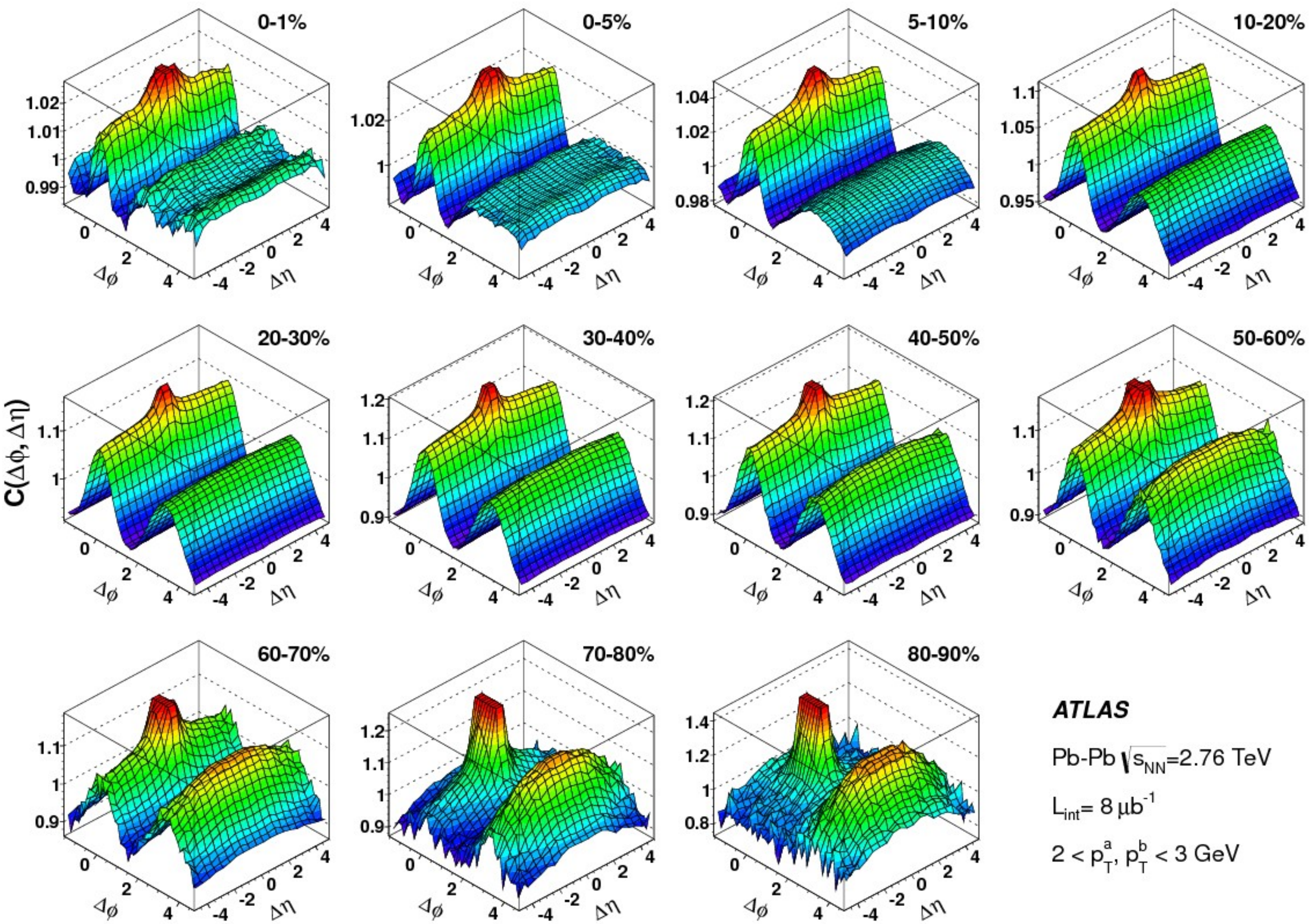

2-Particle Correlations in Pb+Pb

Phys. Rev. C 86, 014907 (2012)

Long and short range structures

Shape of C(Δφ) is well described by the sum of $v_{n,n}$ 2-6 harmonics

$$\frac{dN_{\rm pairs}}{d\Delta\phi} \propto 1 + 2\sum_{n=1}^{\infty} v_{n,n}(p_{\rm T}^{\rm a}, p_{\rm T}^{\rm b}) \cos n\Delta\phi$$

$$v_{n,n} = \langle \cos n\Delta\phi \rangle = \frac{\sum_{m=1}^{N} \cos(n\Delta\phi_m) C(\Delta\phi_m)}{\sum_{m=1}^{N} C(\Delta\phi_m)}$$

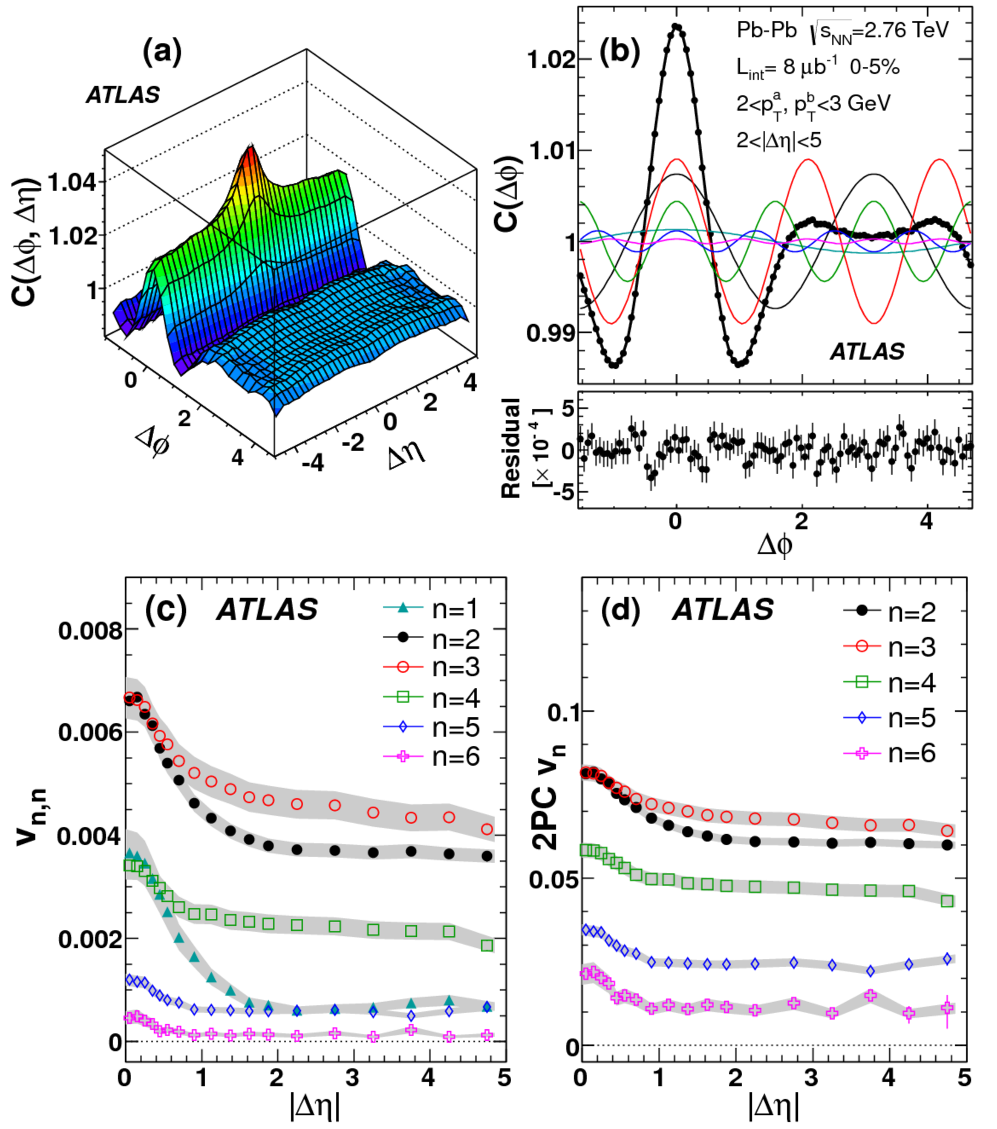

Messages from Global Observables

- Centrality dependence of inclusive multiplicity scales with beam energy.

- Significant harmonic (v_2-v_6) observed in Pb+Pb collisions reflecting the nuclear overlap and fluctuations of the initial nucleon-nucleon positions.

- v_n distributions are not fully consistent with the eccentricity distributions from the Glauber and/or KLN MC models.

- The long range “ridge” and “cone” structures in two-particle correlation function at low p_T can be explained by flow effects.

Electroweak Probes

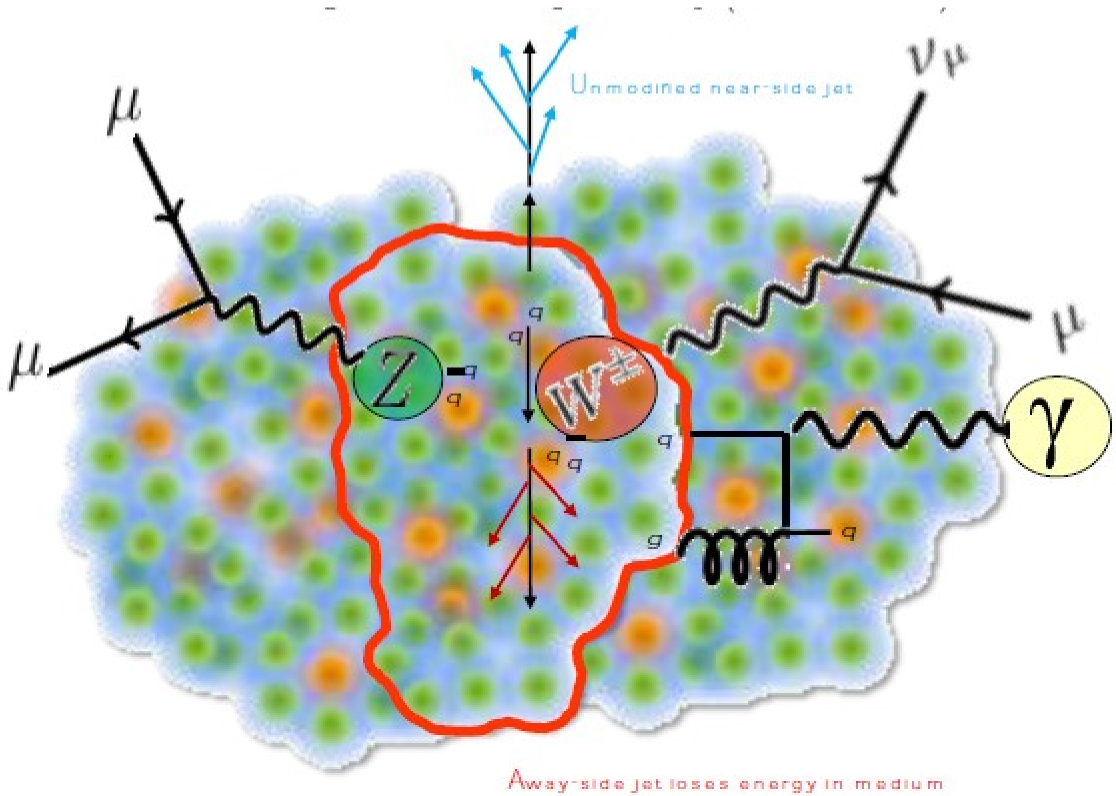

W/Z, photons, are not supposed to interact with QGP. W/Z leptonic decays either.

Can be used as benchmarks for in-medium effects.

Can also be used to check models of collision geometry (Glauber). Their production is expected to scale with number of nucleon-nucleon collisions.

Direct Photons as a Function of p_T

ATLAS-CONF-2012-051

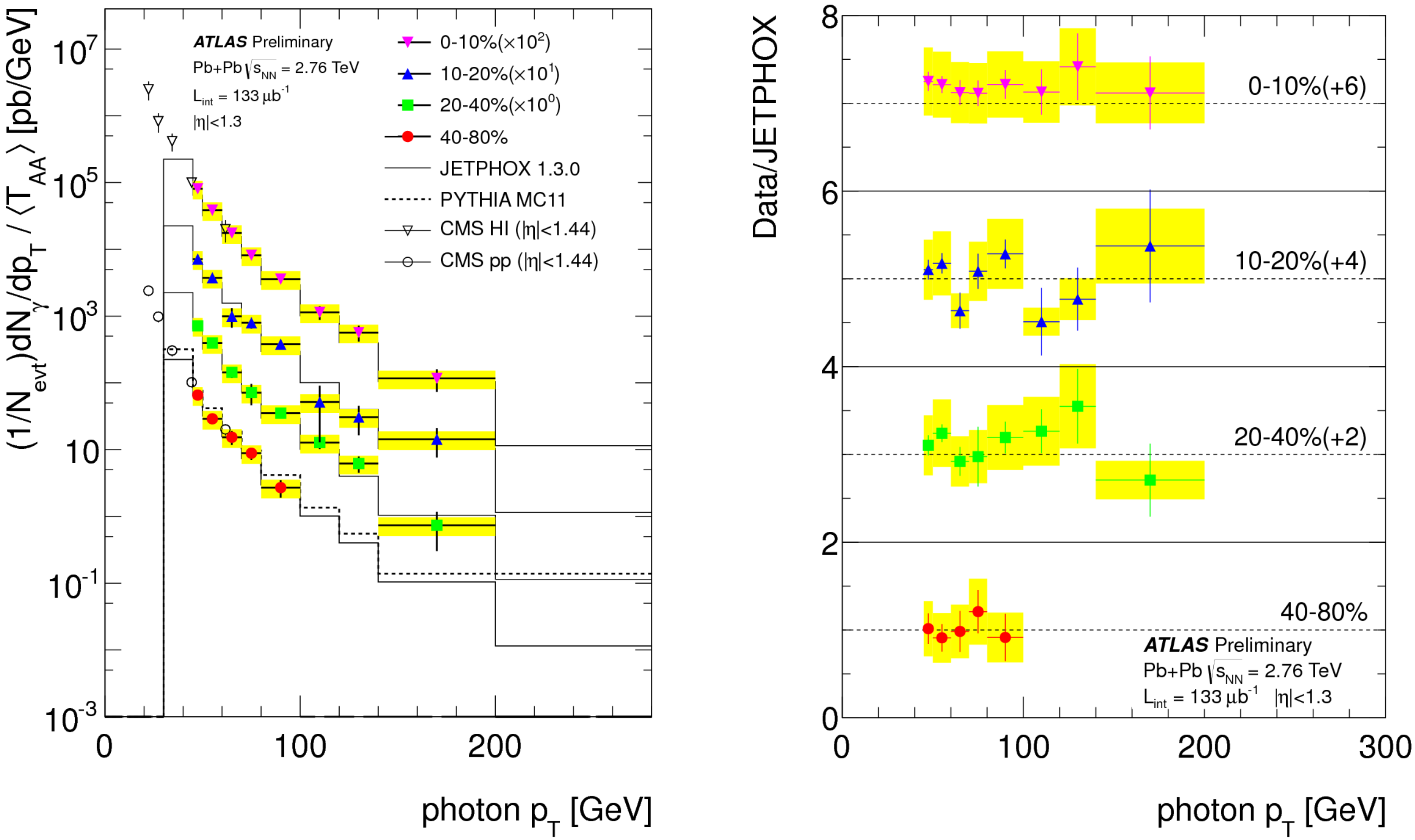

Good agreement with model and CMS results in Pb+Pb and p+p

Z Production

Phys. Rev. Lett 110, 022301 (2013)

Z boson rapidity distribution

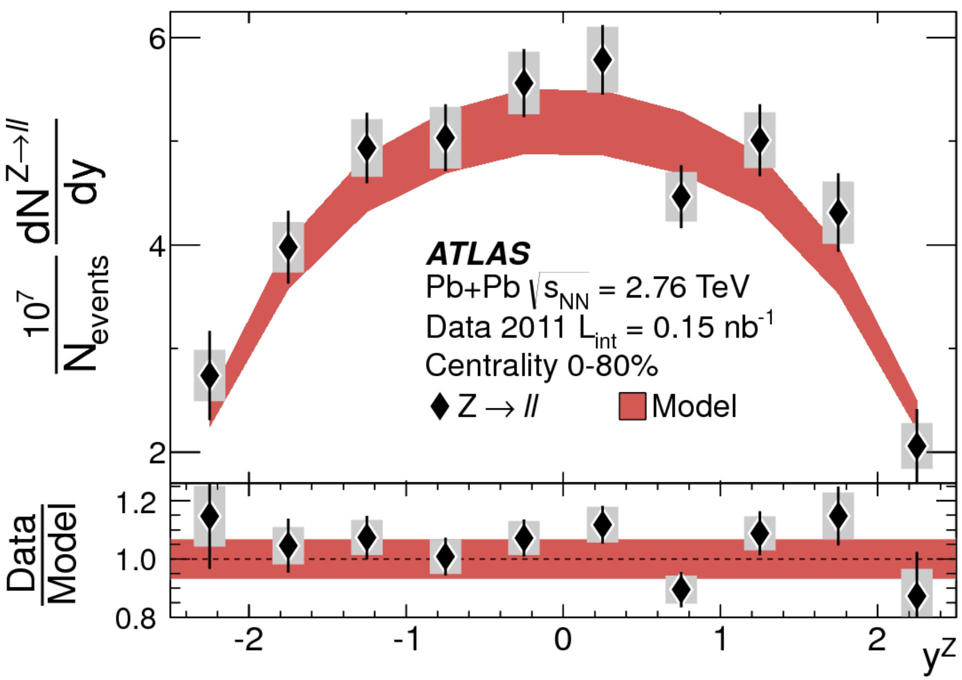

Centrality dependence of Z yield

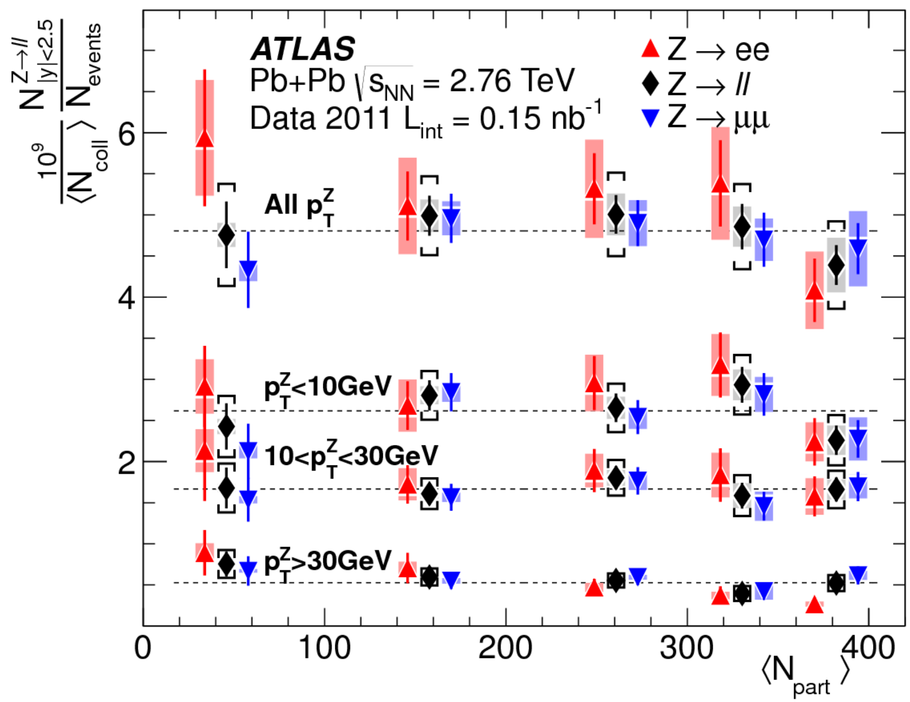

Agreement with PYTHIA normalized to Z→ll cross section in p+p collisions at 2.76 TeV taken from NNLO calculations

Well compatible with binary scaling (validates Glauber)

$W^{\pm}$ as a Function of Muon p_T

ATLAS-CONF-2013-106

W→μν channel (ID+MS combined muons)

Fiducial region: $p_T^{\mu} > 25$ GeV; $p_T^{\nu} > 25$ GeV; $0.1<|\eta_{\mu}|<2.4$; $m_T > 40$ GeV

In Pb+Pb collisions a track-based p_T^{miss} variable is used as a proxy for p_T^{ν}

Reject opposite-sign muon pairs with $m_{\mu\mu} > 66$ GeV (reject Z)

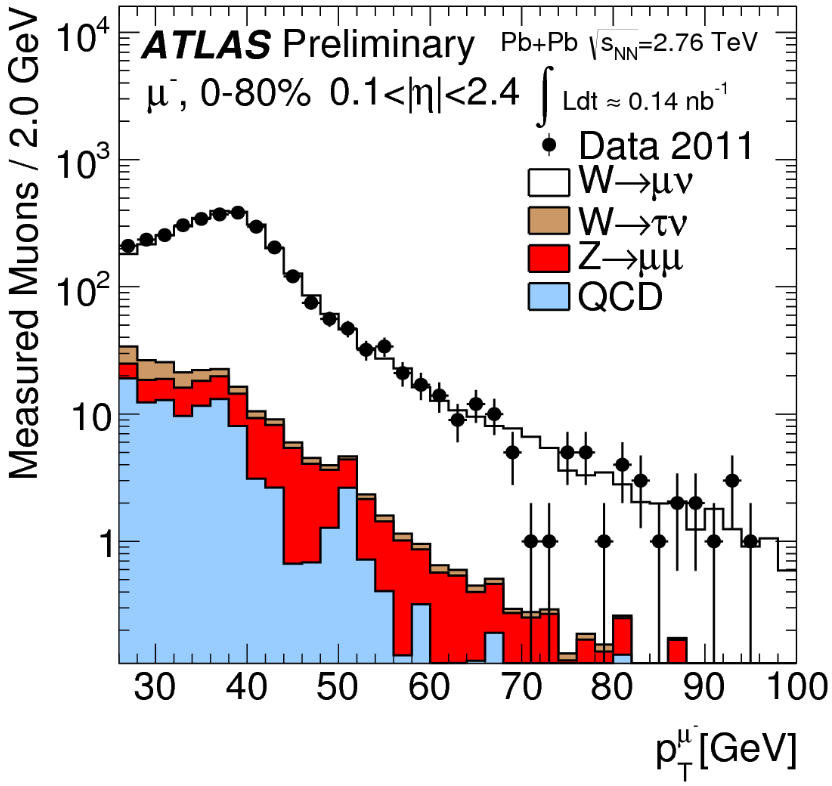

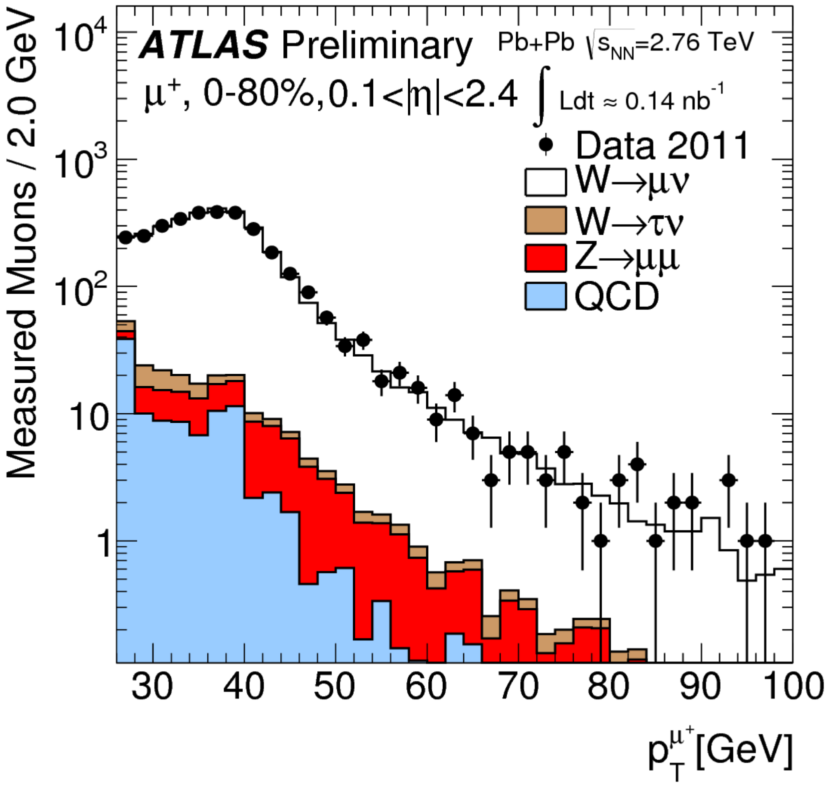

$W^{\pm}$ as a Function of m_T

ATLAS-CONF-2013-106

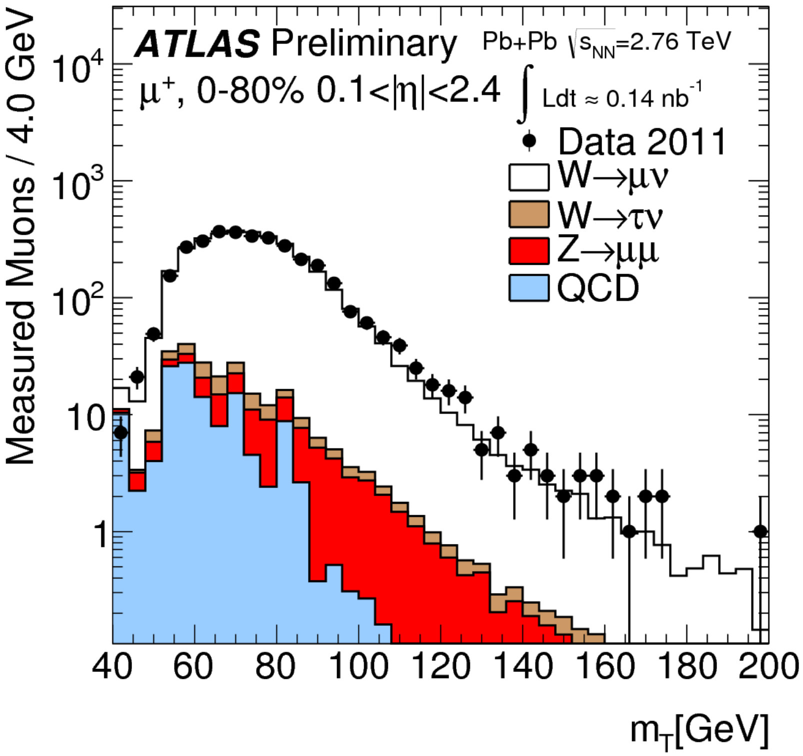

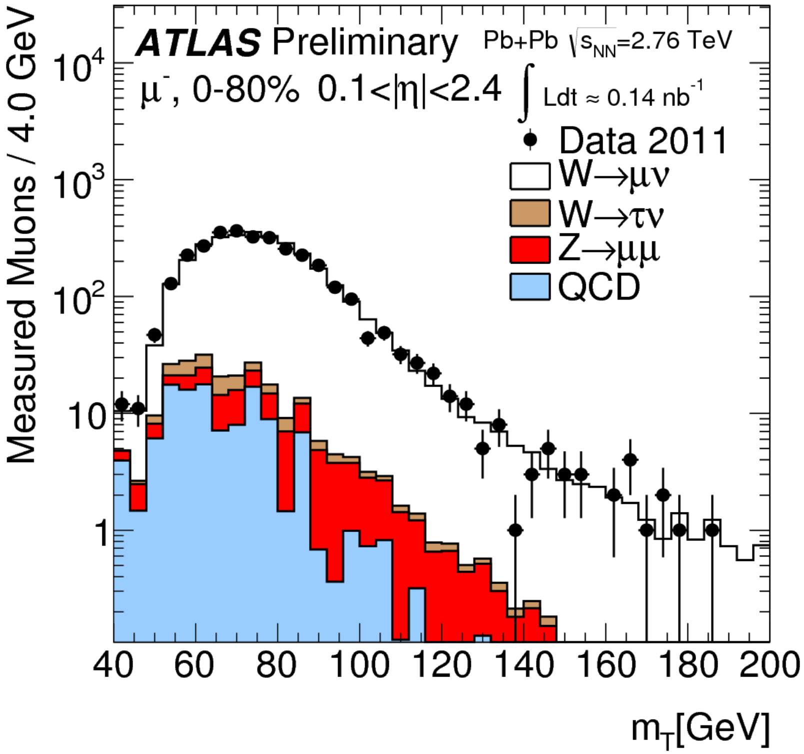

$$m_T = \sqrt{2 p_T^{\mu} p_T^{\text{miss}} (1 - \cos \Delta\phi_{\mu, p_T^{\text{miss}}})}$$

$$\mathbf{p}^{\text{miss}} = \sum_{i=1}^{ntrks} \mathbf{p}_i^{\text{miss}} = -(\mathbf{p}_1 + \mathbf{p}_2 + \ldots \mathbf{p}_{ntrks})$$

- Number of QCD and electroweak background events are normalized to expected number of events

- W→μν MC normalized to the number of background subtracted events in the data

$W^{\pm}$ Bosons per Binary Collisions

ATLAS-CONF-2013-106

5487±96(stat)±86(syst) W^+

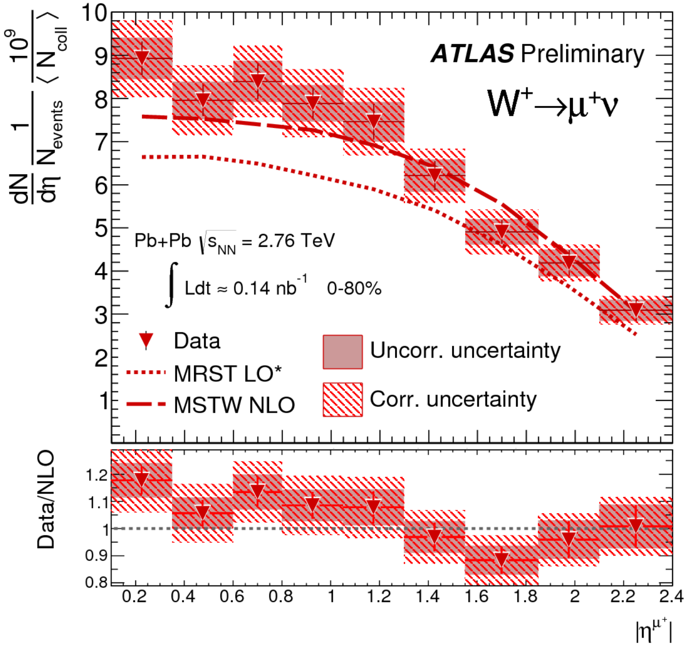

5262±95(stat)±83(syst) W^-

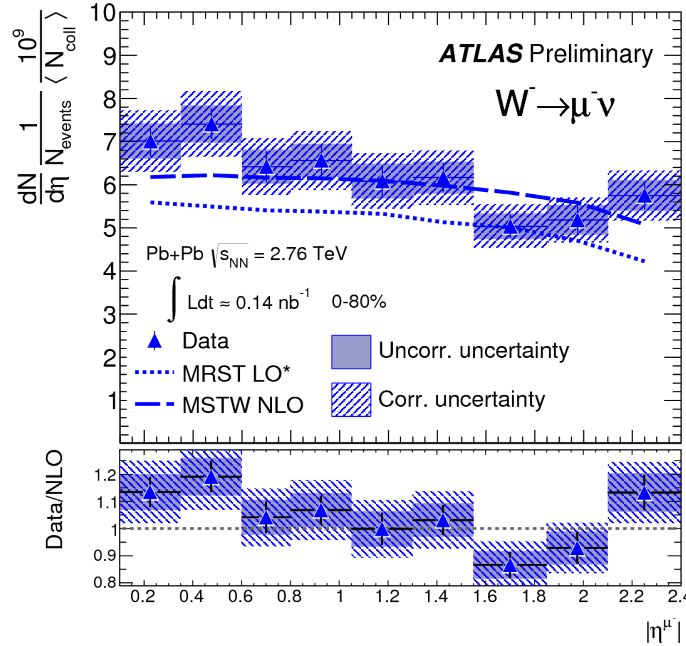

Difference between W^+ and W^- at large η is due to spin conservation:

$W^{\pm}$ at large η produced from high-x (valence) quarks

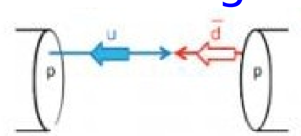

$u\bar{d} \rightarrow W^+$ more W^+ than W^- in p+p collisions

$d\bar{u} \rightarrow W^-$ more W^- than W^+ in Pb+Pb collisions

μ^- is boosted in direction of $W^- \rightarrow$ more μ^- at large η

LO prediction underestimates the data. NLO agrees much better.

Muon Charge Asymmetry

ATLAS-CONF-2013-106

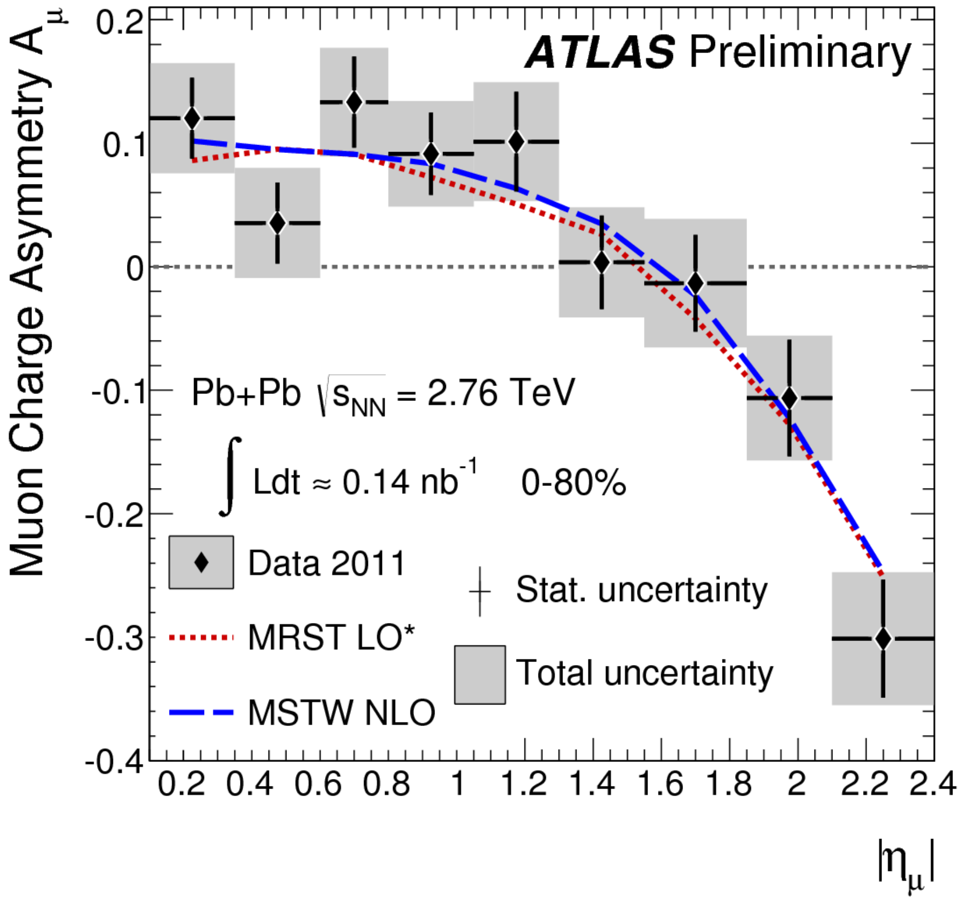

$$A_\mu = \frac{d\sigma_{W^+\to\mu^+}/d\eta_\mu - d\sigma_{W^-\to\mu^-}/d\eta_\mu}{d\sigma_{W^+\to\mu^+}/d\eta_\mu + d\sigma_{W^-\to\mu^-}/d\eta_\mu}$$

Data agree with both LO and NLO predictions

No visible PDFs modifications (yet)

Messages from EW Probes

- Photons, Z and $W^{\pm}$ productions consistent with simple scaling with number of nucleon-nucleon collisions, N_{coll}

- They are a precious reference for in-medium QCD effects of other observables, as jet suppression.

- No visible modifications of nuclear PDFs within uncertainties

Jets in Pb+Pb Collisions

"Jet Quenching" is the modification of parton showers in the QGP

Observables at LHC (so far):

- Dijet Asymmetry, Acoplanarity
- Jet energy loss through correlation with colour neutral probes (Z and photons)
- Differential inclusive jet suppression
  - Dependence on centrality and Δφ
  - Dependence on jet size
- Jet structure and properties of quenched jets
  - Distributions of particles within jets
  - Distributions of particles p_T and Z

More in future: sensitivity to quark/gluon jets;
heavy flavour jets...

Jet Reconstruction

• Jets are reconstructed using anti-k_T algorithm with cone sizes R=0.2, 0.3, 0.4 and 0.5

• Inputs are 0.1x0.1 ($\Delta\eta x \Delta\phi$) calorimeter towers or ID tracks

• Average background estimated event-by-event per calorimeter sampling layer and per 0.1 η strip and subtracted (excluding jets and accounting for elliptic flow)

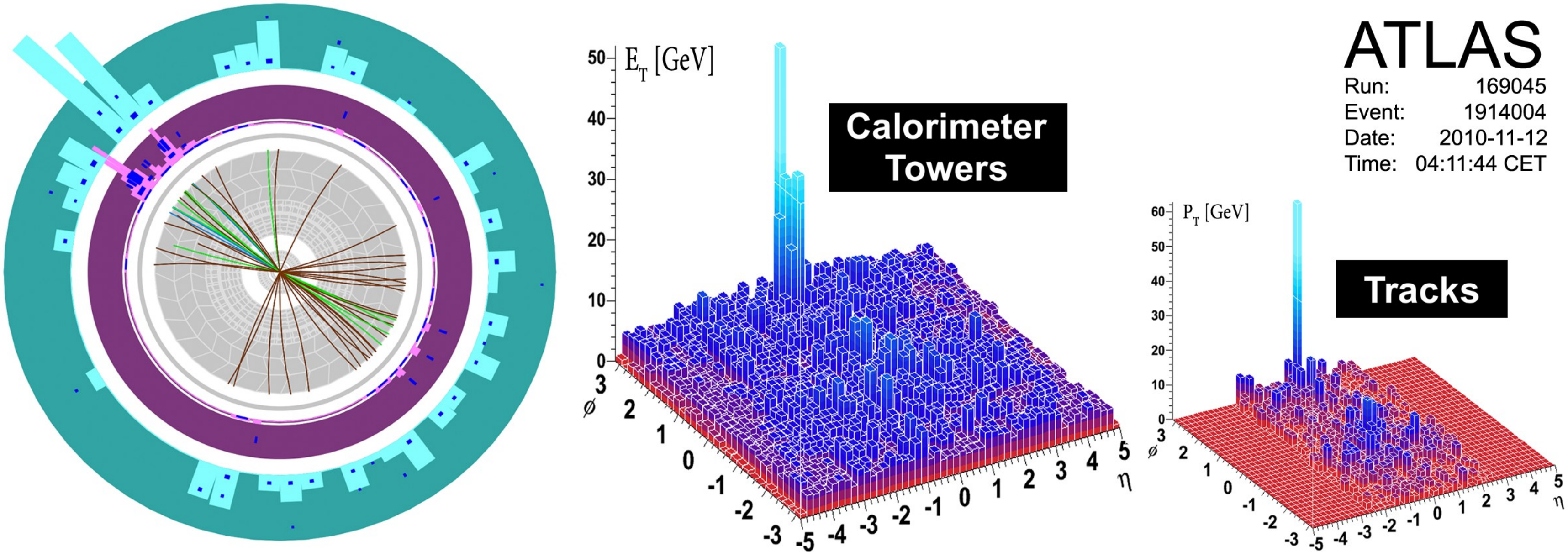

Di-jet Asymmetry

Enhancement of asymmetric di-jets, relatively to p+p and PYTHIA+HIJING

→ first indication of jet suppression at LHC

$$A_J = \frac{E_{T1} - E_{T2}}{E_{T1} + E_{T2}}$$

$E_{T1} > 100\,GeV$

$E_{T2} > 25\,GeV$

$|\eta| < 2.8$

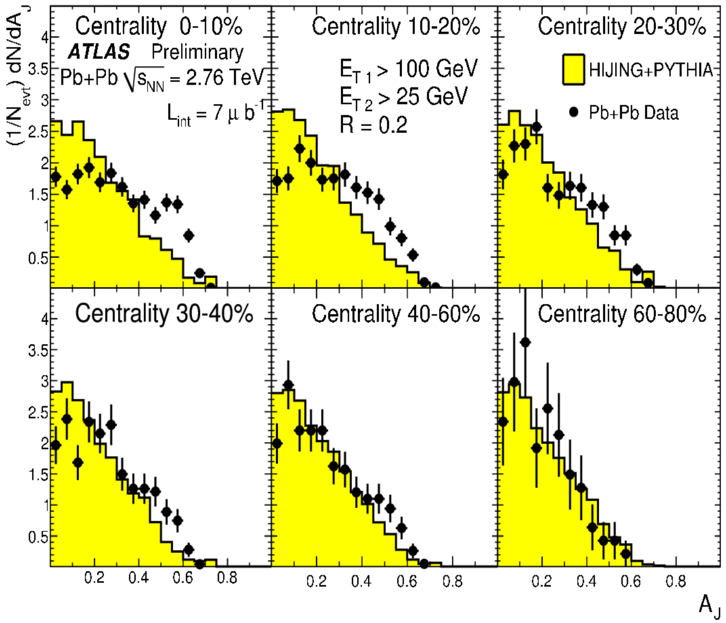

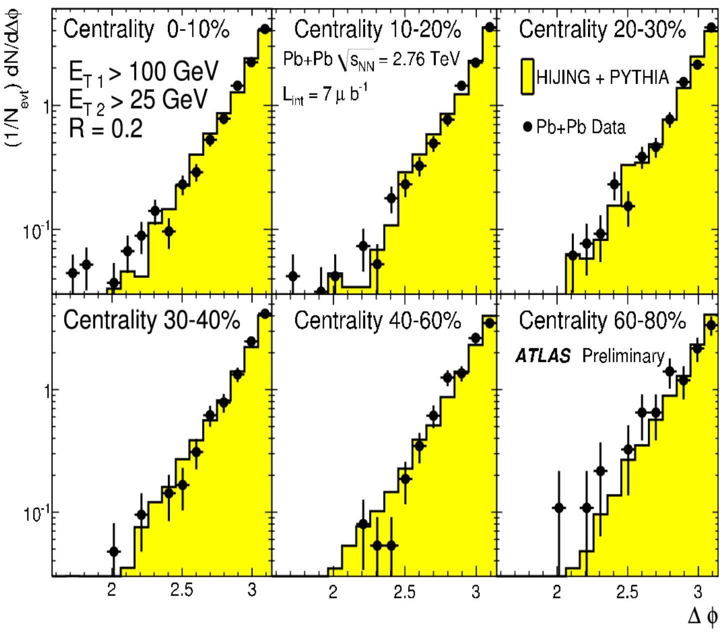

Δφ = π acoplanarity remains, while A_J is changing

PYTHIA+HIJING does not know anything about “jet quenching”

Photons+jets

Photon+jet yield as a function of momentum fraction

ATLAS-CONF-2012-121

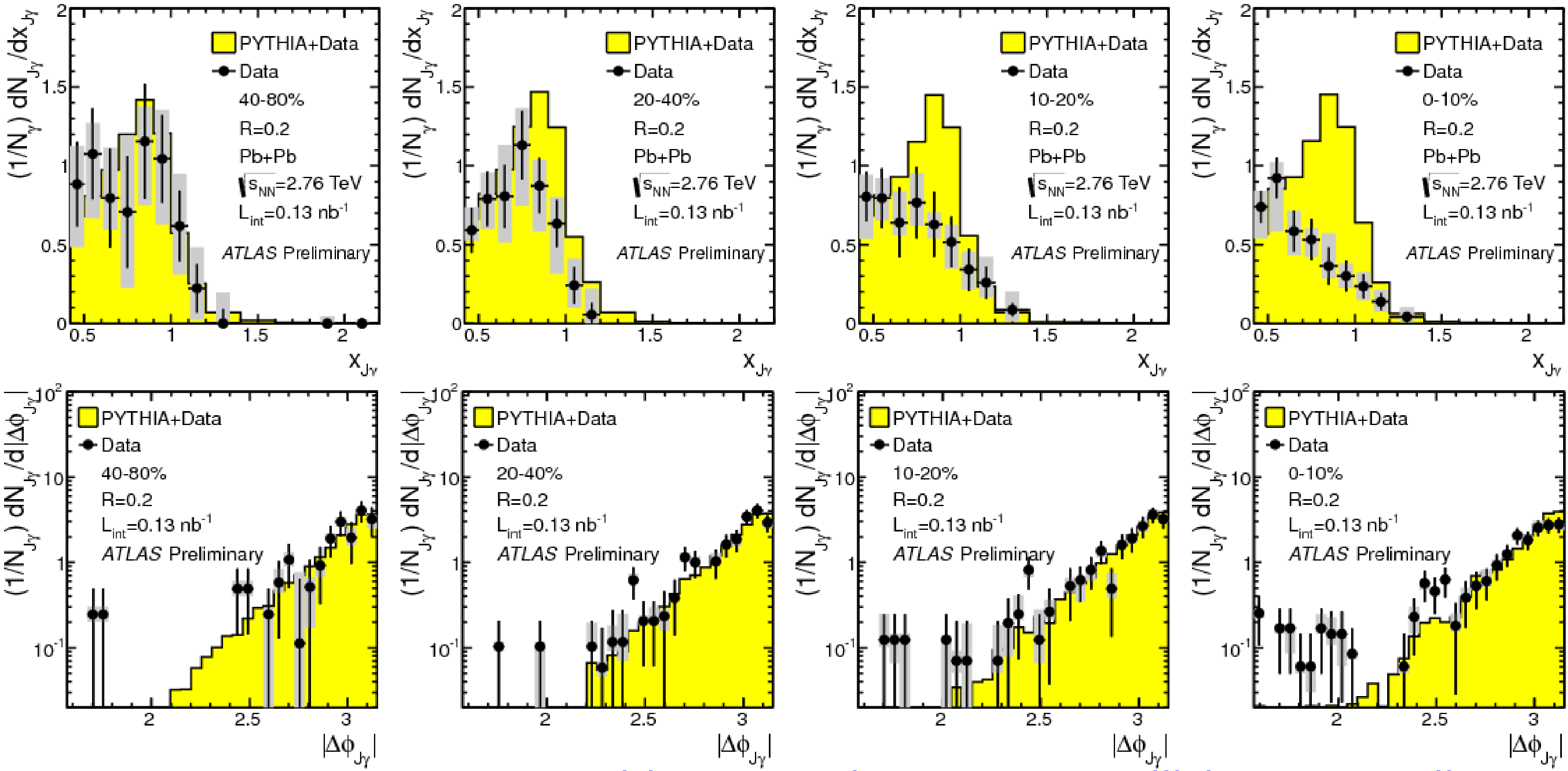

$$x_{j\gamma} = \frac{p_T^{jet}}{p_T^{\gamma}}$$

Agreement with PYTHIA decreases as collision's centrality increases, indicative of jet energy loss.

But..., they remain back-to-back.

Z+jets

ATLAS-CONF-2012-119

Z+jet yield as a function of momentum fraction

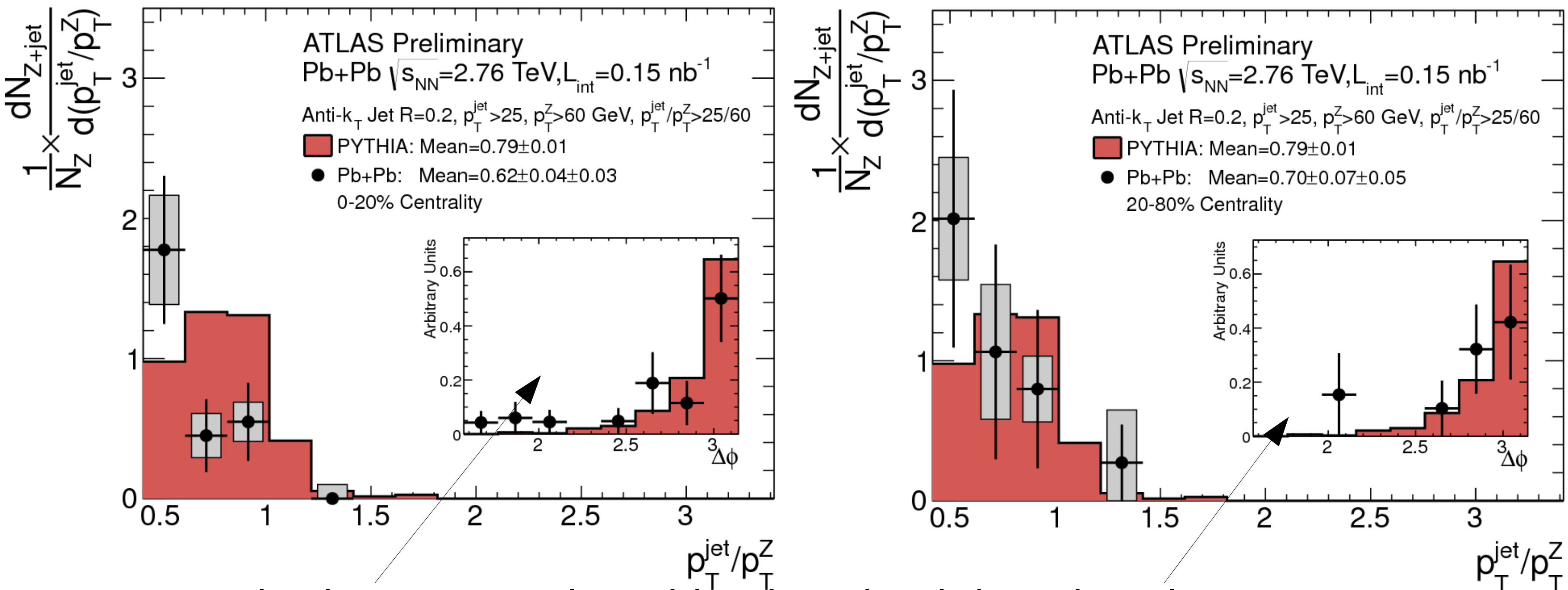

Jets and Z bosons produced back-to-back in azimuth

Agreement with PYTHIA decreases as collision's centrality increases, but more data needed

R_{CP} versus p_T and Centrality

Phys. Lett. B 719 (2013) 220-241

$$R_{CP} = \frac{1/N_{coll}^{cent}}{1/N_{coll}^{periph}} \frac{1/N_{evnt}^{cent}\, dN/dE_T}{1/N_{evnt}^{periph}\, dN/dE_T}$$

“periph” is the jet yield in the 60-80% centrality interval

R=0.4

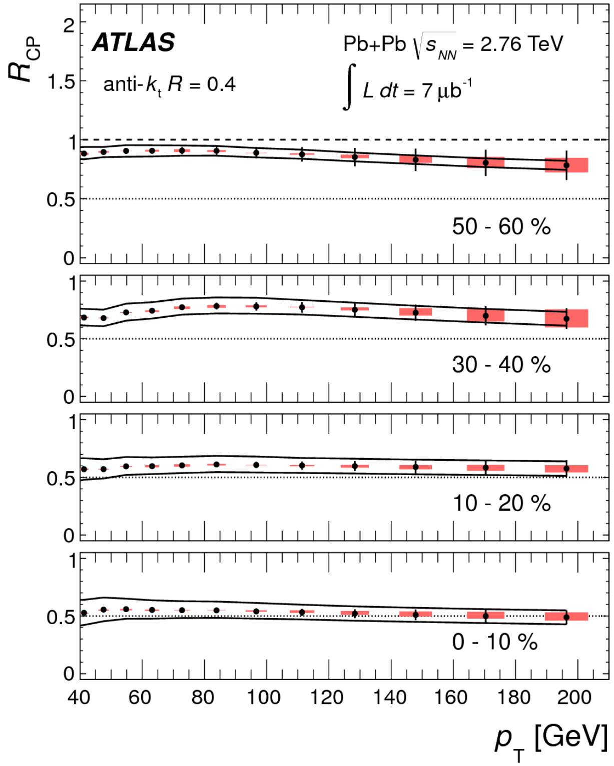

R=0.2

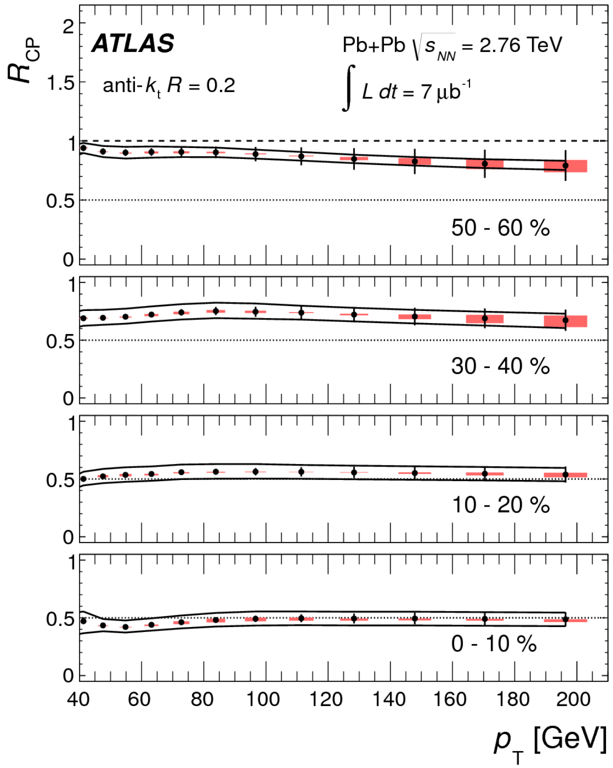

Increasing jet suppression with centrality, up to a factor of 2 in the most central collisions, well beyond statistical and systematic errors

R_{CP} – Dependence on Jet Size

Ratios of R_{CP} to R_{CP} with R=0.2

Phys. Lett. B 719 (2013) 220-241

Measure relative suppression with respect to most suppressed jet cone size (R=0.2)

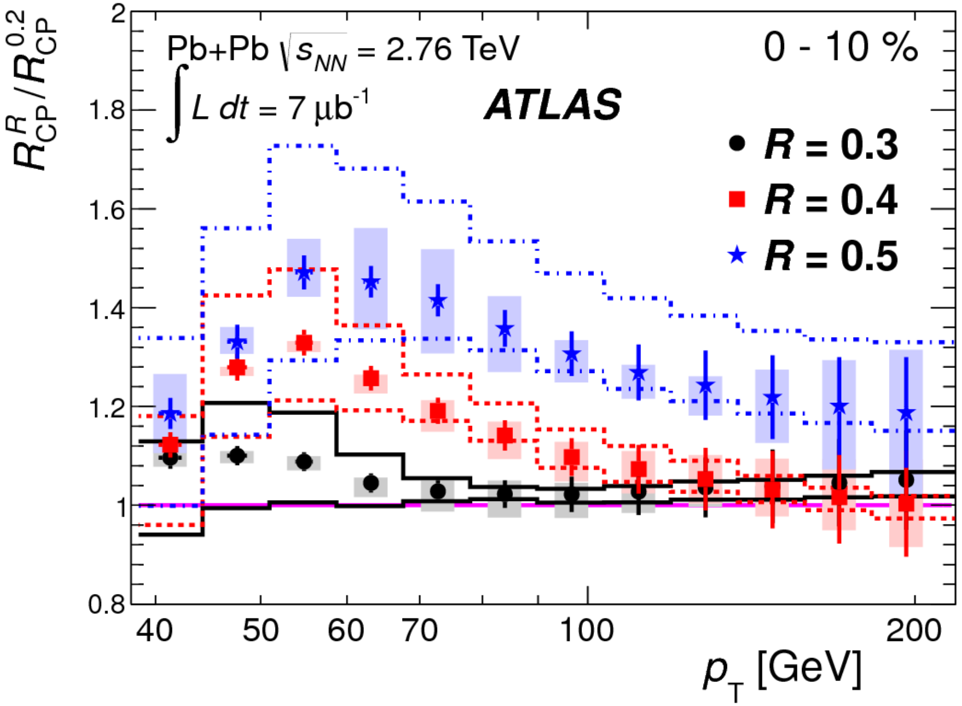

Expectations from model

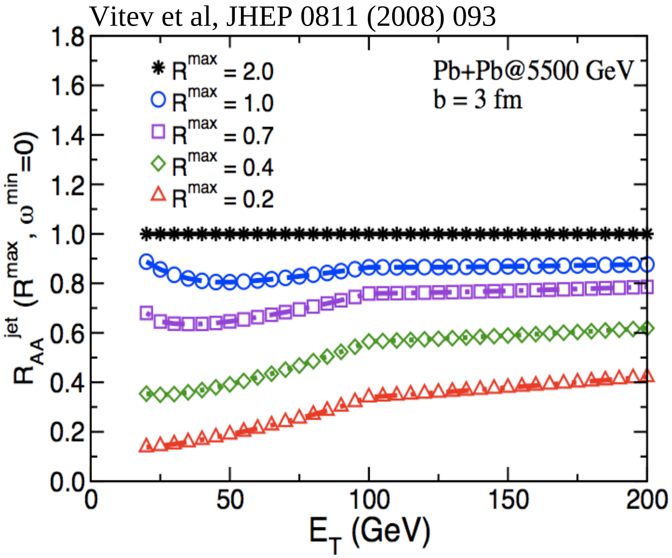

Variation with jet size is significant

Statistical correlations between different R propagated

Correlated systematics between different R cancel out

Azimuthal Angle Dependence

Jets measured at different azimuthal angles with respect to the reaction plane, $\Delta\varphi=\varphi_{jet} - \Psi_2$, originate in partons that traverse different path lenghts in medium.

$$\frac{dN}{d\phi} \propto 1 + 2v_2 \cos 2(\phi - \Psi_2)$$

Phys. Rev. Lett 111, 152301 (2013)

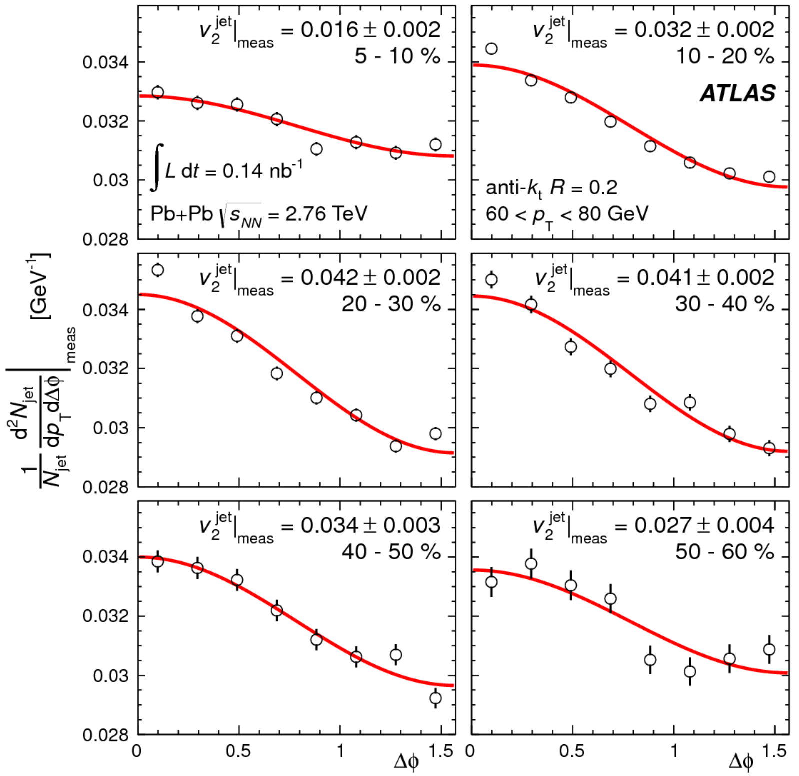

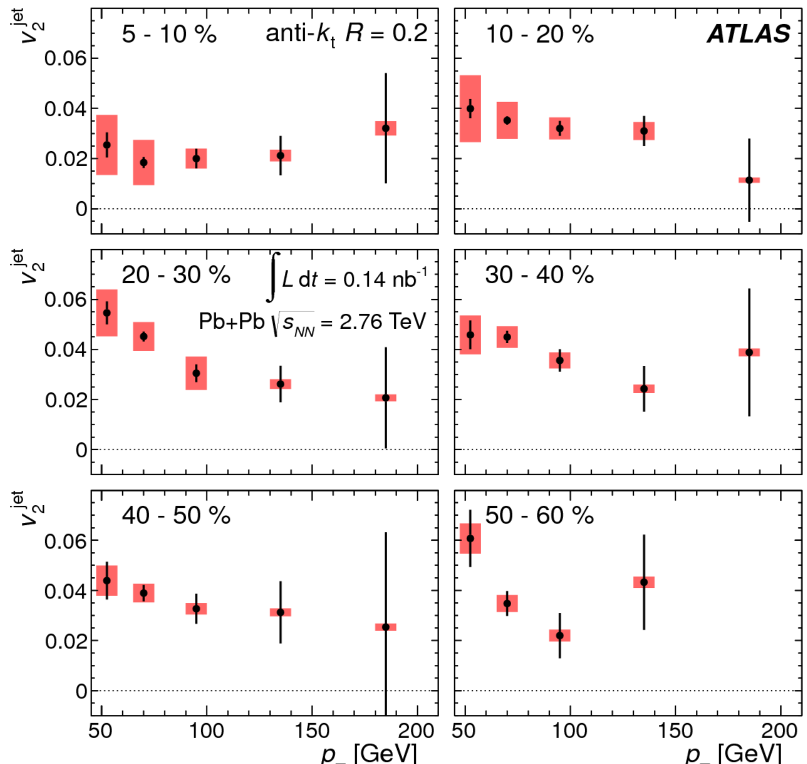

- Jets produced in the direction of the event plane are less suppressed
- Weak p_T depence of v_2

Jet Structure – D(z)

ATLAS-CONF-2012-115

D(Z) measures the p_T of the fragments inside the jet

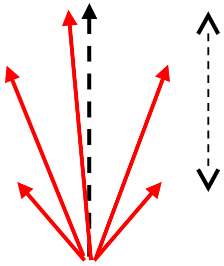

$$z \equiv \left(\frac{p_{T,had}}{E_{T,jet}}\right) \cos \Delta R$$

Expectations from model

Armesto et al, JHEP 0802 (2008) 048

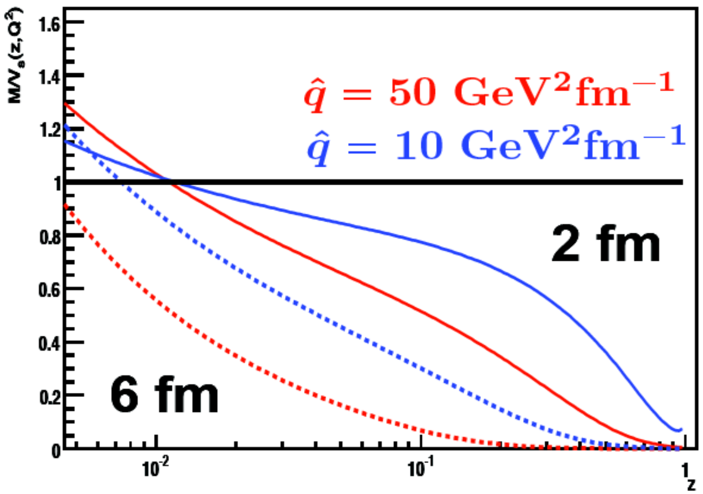

Ratio = $D_{0\text{-}10\%}$ / $D_{60\text{-}80\%}$

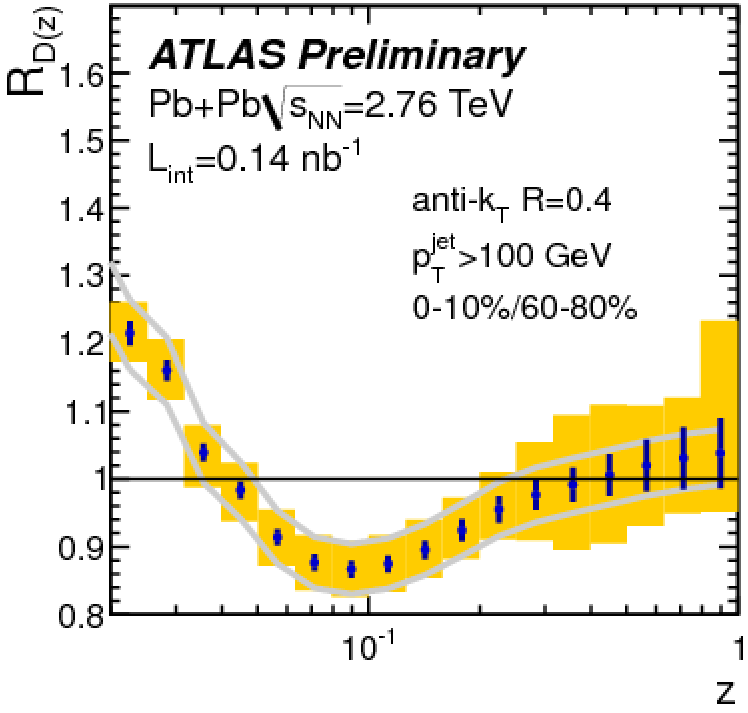

- ~20% enhacement at low z
- ~20% reduction at intermediate z
- expectations at high z not confirmed

Jet Production in p+Pb

$$R_{CP} = \frac{1/N_{coll}^{cent}}{1/N_{coll}^{periph}} \frac{1/N_{evnt}^{cent}\, dN/dE_T}{1/N_{evnt}^{periph}\, dN/dE_T}$$

ATLAS-CONF-2013-105

"periph" is the jet yield in the 60-90% centrality interval

- R_{cp} is suppressed (<1) in all rapidities.
- At fixed y* the suppression increases systematically with p_T.
- The suppression increases as centrality increases.

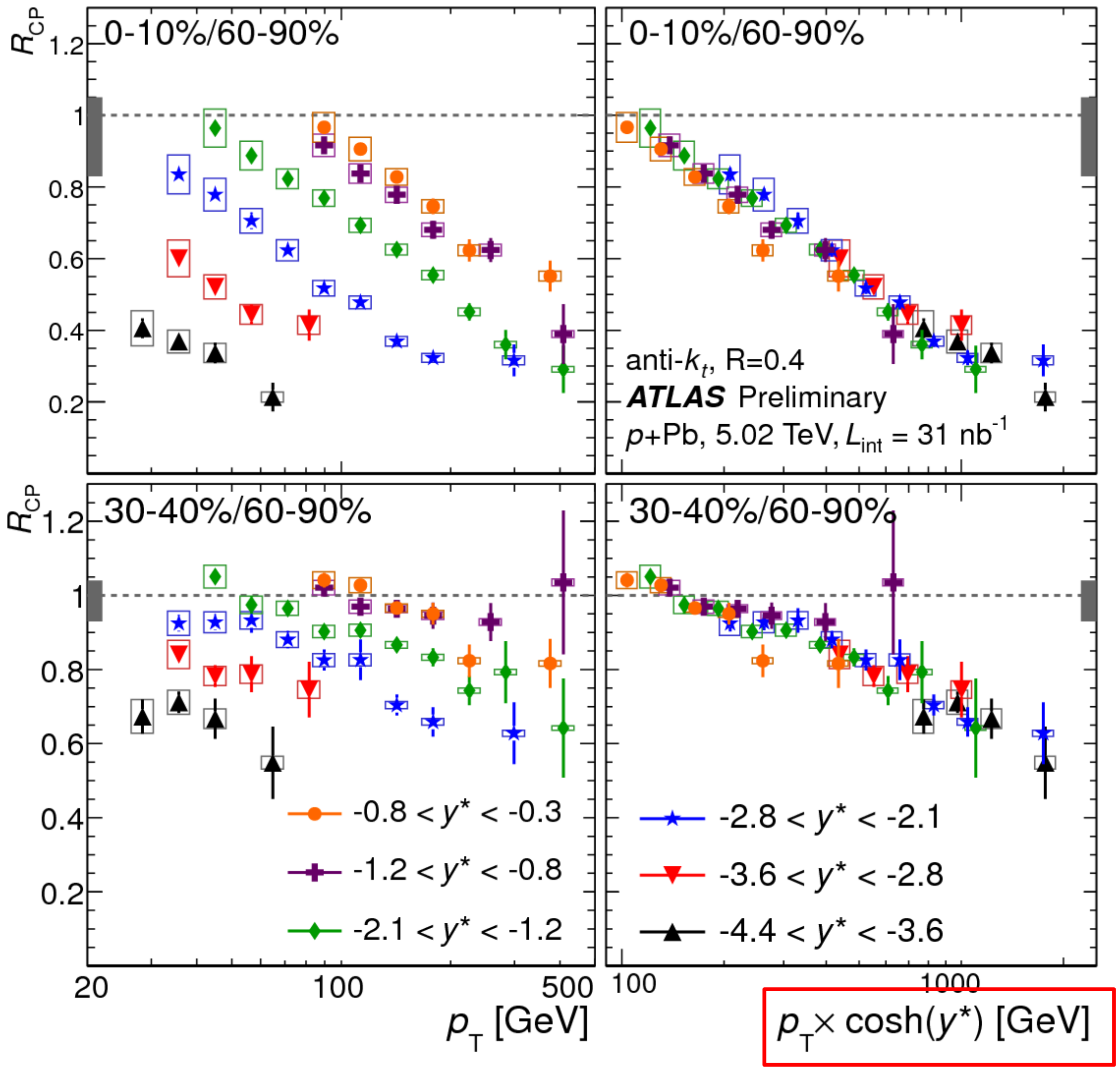

Messages from Jets

- Di-jet balance in peripheral collisions well compatible with non-quenching based MC;

  Di-jet asymmetry increases with increasing centrality.

  No broadening of Δφ.

  The same conclusions for photon+jet and Z+jet balance.
- Jet production suppressed by a factor of 2 in central collisions.
- R = 0.2 jets more suppressed, as expected.
- Expectations of D(z) modifications at large z not confirmed.
- Jets produced in the direction of the event plane are less suppressed.
- In p+Pb collisions the R_{cp} at all rapidities studied is consistent with being a function of the total jet energy only.

Backup

2010 and 2011 Pb+Pb Run

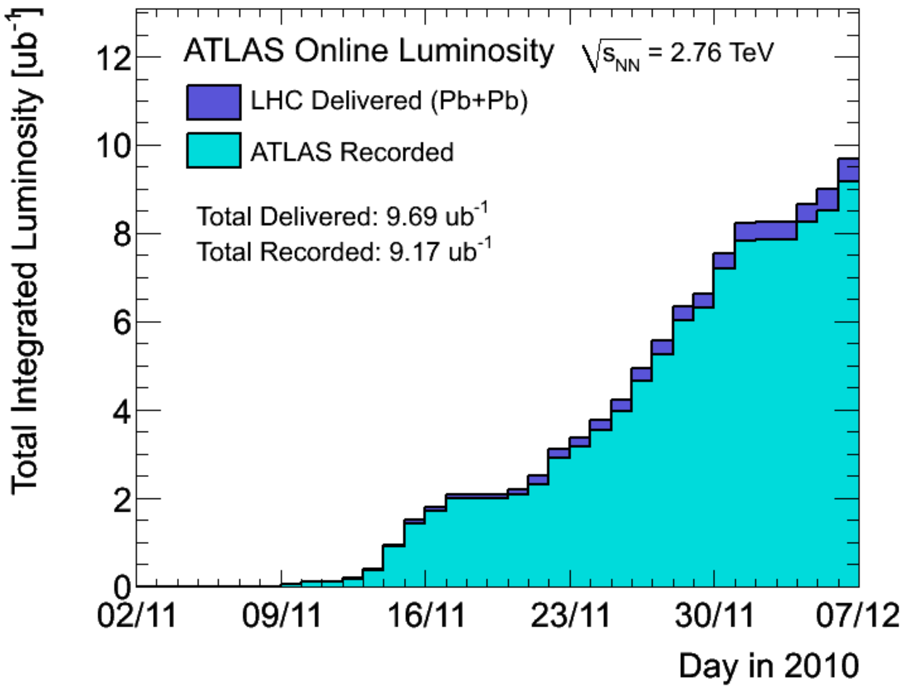

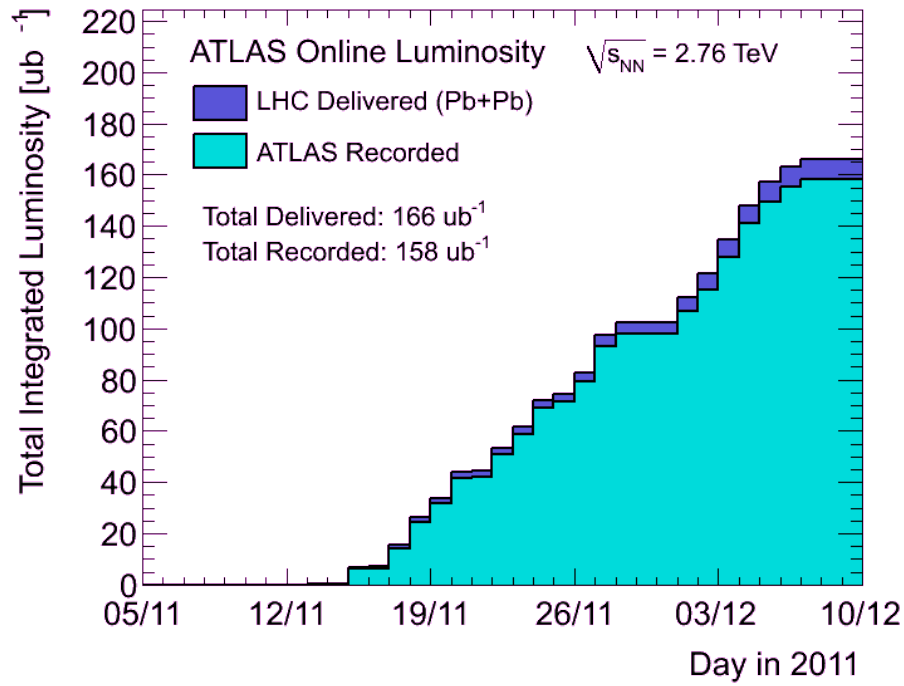

Fraction of data passing data-quality criteria > 99%

In 2010

Inner Tracking Detectors			Calorimeters				Muon Detectors			
Pixel	SCT	TRT	LAr EM	LAr HAD	LAr FWD	Tile	MDT	RPC	CSC	TGC
99.7	100	100	99.2	100	100	100	100	99.6	100	100

Luminosity weighted relative detector uptime and good quality data delivery during 2010 stable beams in PbPb collisions at $\sqrt{s_{NN}}$=2.76 TeV between November 8th and 17th (in %).

Multiplicity in p+Pb collisions

Deviations from simple geometrical expectations due to:

- Shadowing (suppression of yields at small p_T)

    - modifications of nuclear PDFs
    - parton saturation at low-x

- Cronin effect (enhancement at intermediate p_T)

    - k_T broadening due to multiple scattering

- Possible energy loss in “cold nuclear matter”

Baseline to understand Pb+Pb collisions

Jet Reconstruction

- Underlying event estimated and subtracted for each longitudinal layer and for 100 slices of $\Delta\eta$ = 0.1:

$$E_{T,subt}^{cell} = E_T^{cell} - \rho \, x A^{cell}$$

ρ is energy density estimated event-by-event from average over $0<\varphi<2\pi$

- Two methods to avoid biasing ρ due to jets

  1 - Sliding window exclusion
  2 - Exclude cells in jets satisfying

$$D = E_{T,max}^{tower} / \langle E_T^{tower} \rangle > 5$$

- For R = 0.4, add an iteration step to ensure jets with E_T>50 GeV are always excluded from ρ estimate
- Correct for underlying event v_2

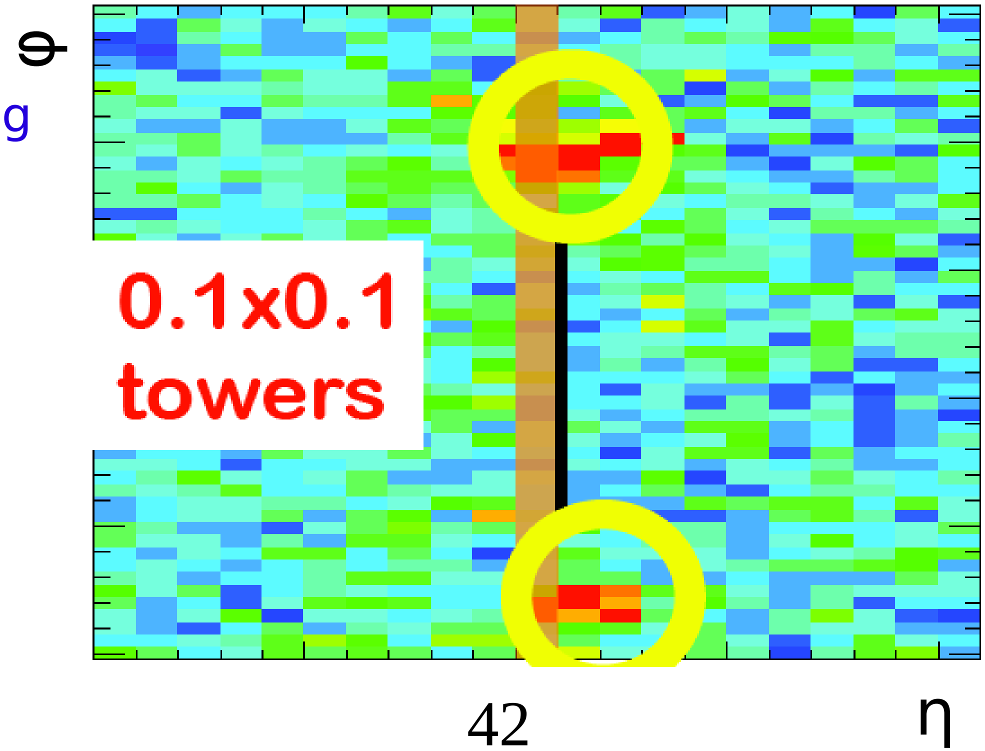

Calorimeter fluctuations

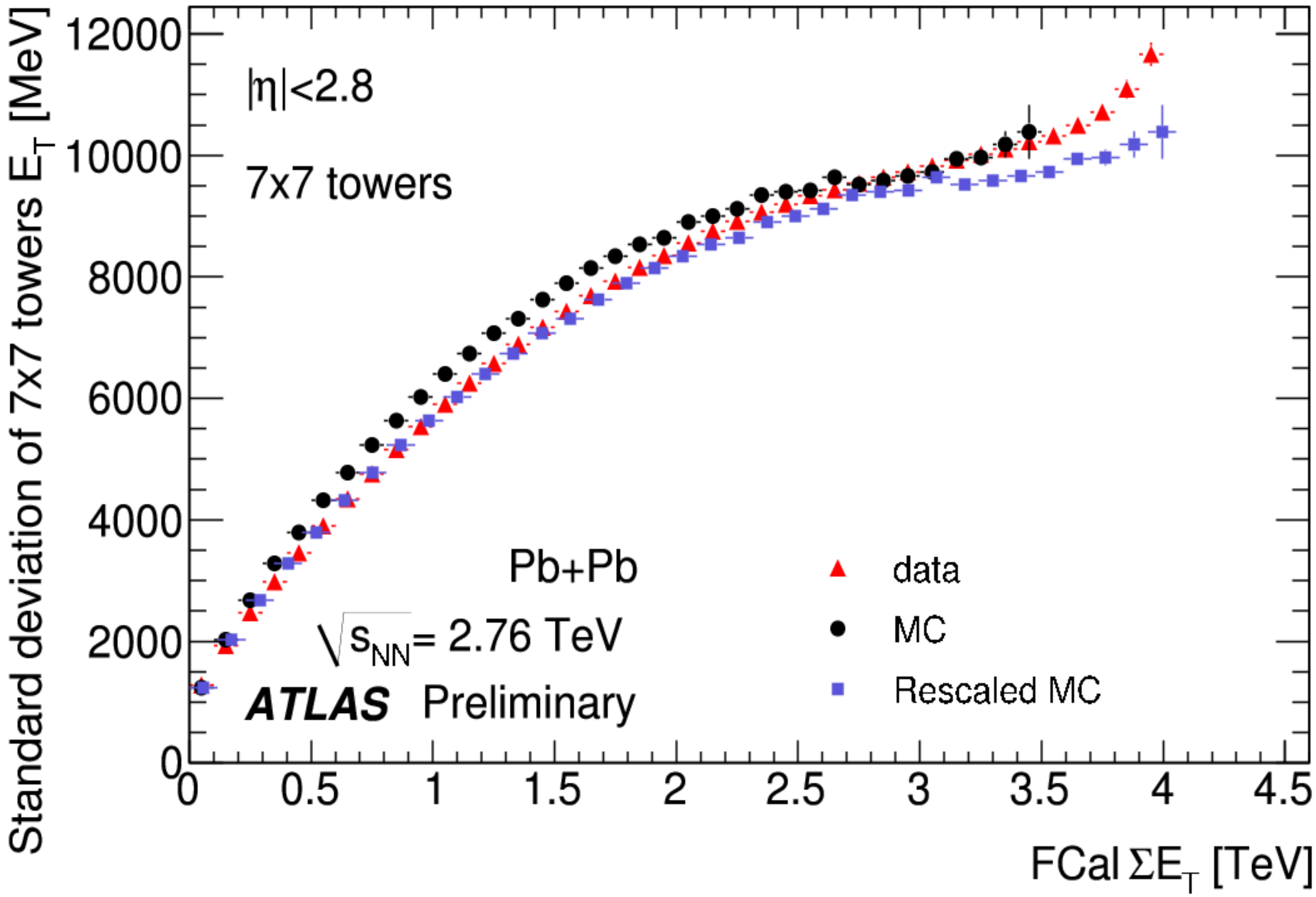

Comparison of the per-event standard deviation of summed ET for 7X7 groups of towers between Pb+Pb data and the HIJING+GEANT Monte Carlo simulated events as a function of FCal Σ ET. The Monte Carlo results are shown with and without the rescaling of the FCal ET values.

Jet Energy Resolution

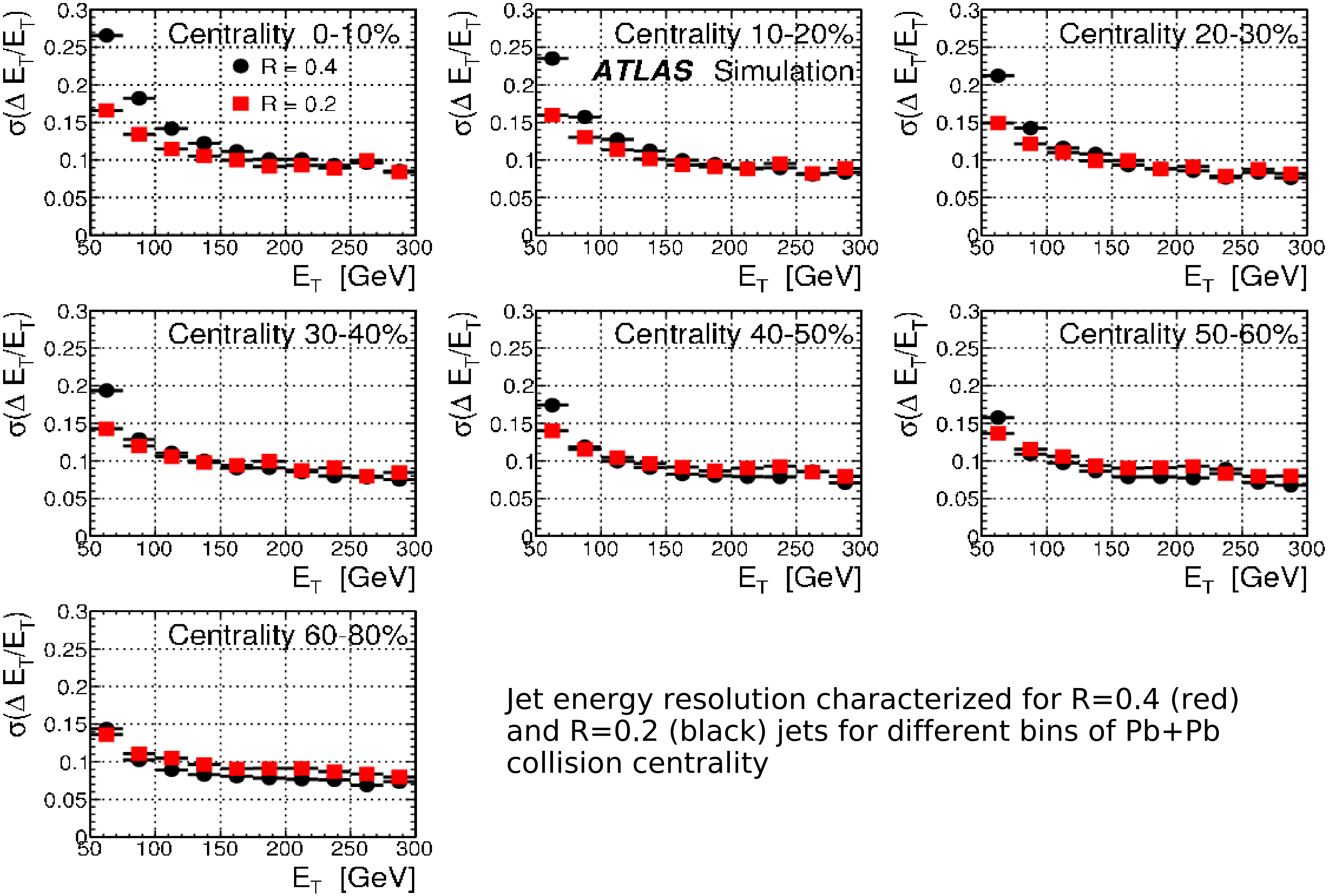

Jet energy resolution characterized for R=0.4 (red) and R=0.2 (black) jets for different bins of Pb+Pb collision centrality

Jet Energy Resolution

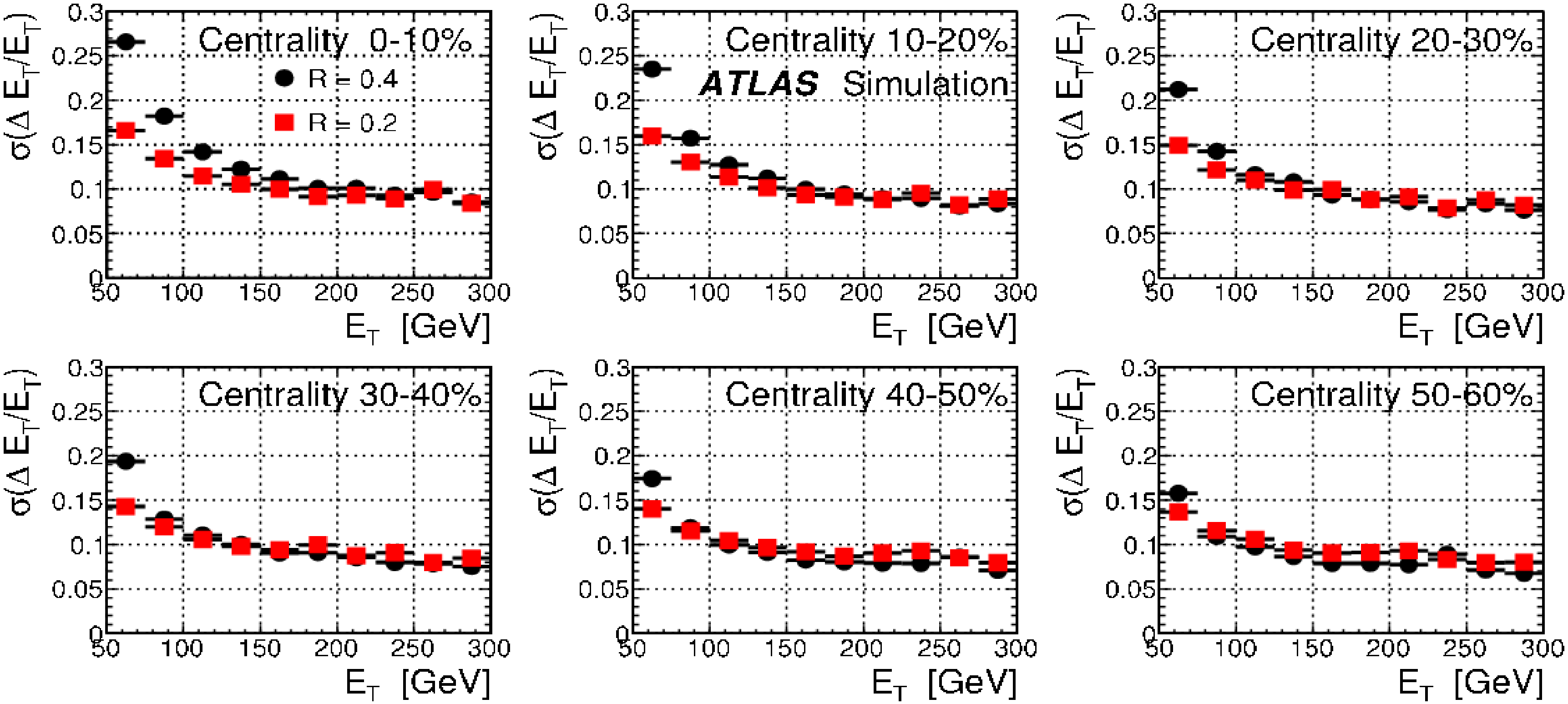

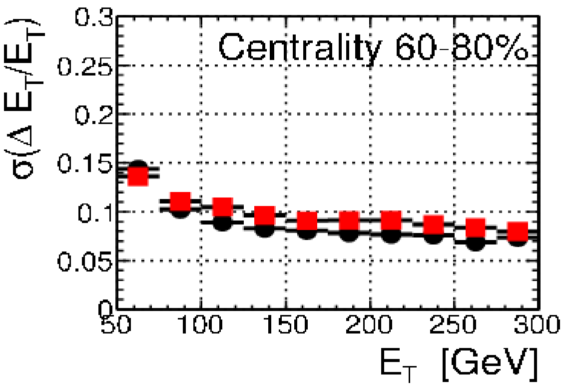

Jet energy resolution characterized for R=0.4 (red) and R=0.2 (black) jets for different bins of Pb+Pb collision centrality

Tracking Efficiency

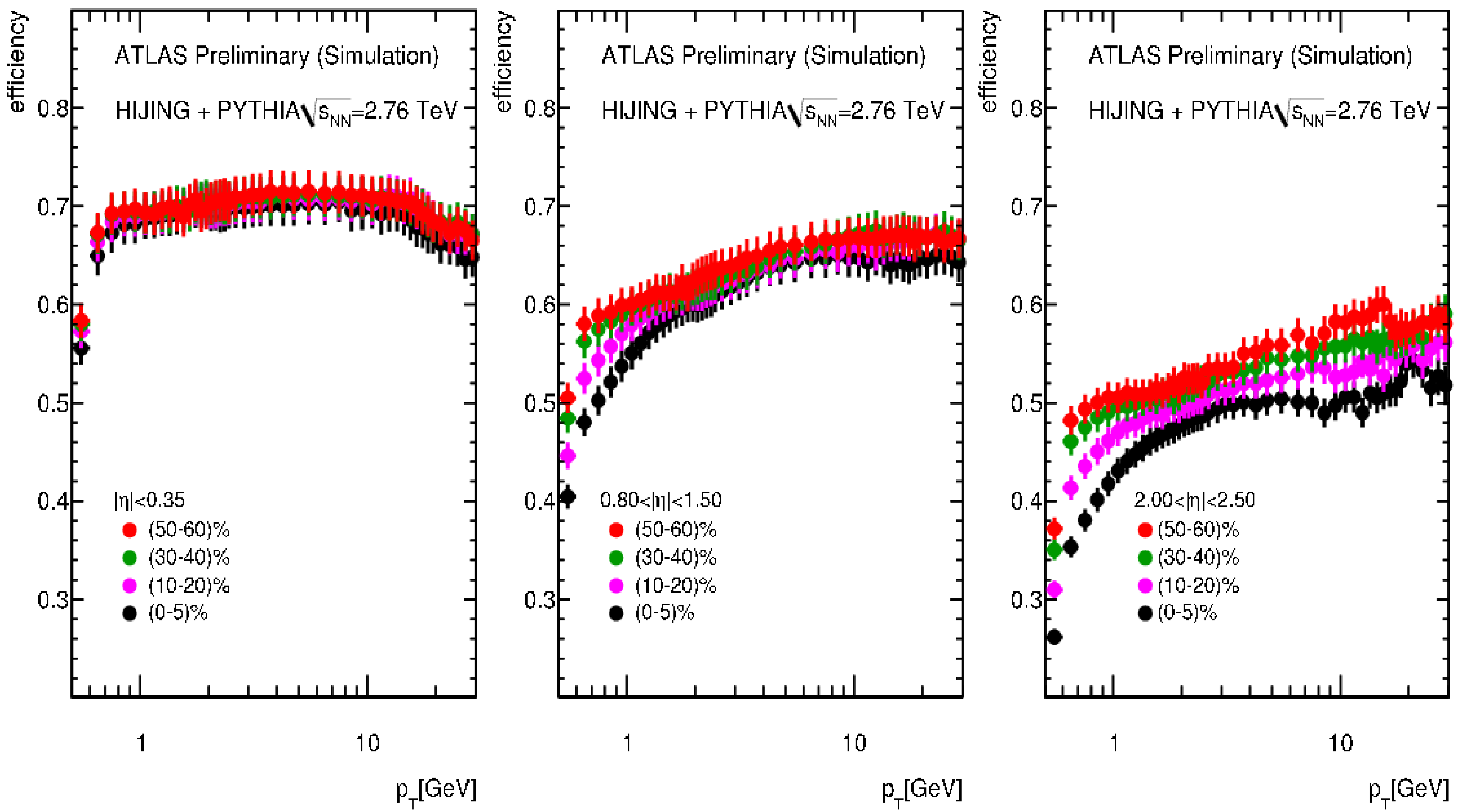

Tracking efficiency calculated from the minimum-bias HIJING and HIJING+jet samples.

Jets in Pb+Pb Collisions

Expectations from models:

- Medium-induced radiation may cause energy deposition outside jet cone

- Predictions of radiative energy loss suggest energy can be recovered by expanding jet cone

Vitev et al, JHEP 0811 (2008) 093

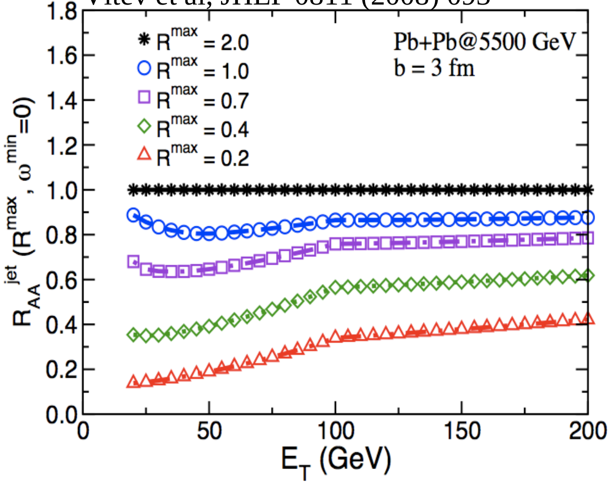

- High z region of fragmentation function sensitive to medium induced radiation

Armesto et al, JHEP 0802 (2008) 048